

# New $^{40}\text{Ar}/^{39}\text{Ar}$ age constraints on the timing of magmatic events in the Panagyurishte region, Bulgaria

ANDREA B. RIESER<sup>1,\*</sup>, FRANZ NEUBAUER<sup>1</sup>, ROBERT HANDLER<sup>1</sup>, SVETLANA H. VELICHKOVA<sup>1,2</sup> & ZIVKO IVANOV<sup>2</sup>

**Key words:** collapse basin, arc magmatism, extension, Cretaceous,  $^{40}\text{Ar}/^{39}\text{Ar}$ -dating, Srednogorie

## ABSTRACT

Amphibole and mica  $^{40}\text{Ar}/^{39}\text{Ar}$  ages have been determined from Late Cretaceous plutonic and volcanic successions from the Panagyurishte region (Bulgaria), which is part of the calc-alkaline to alkaline Banatite belt spreading from the Apuseni Mountains to the Black Sea and hosting world-class Cu-Au-deposits. The post-collisional magmatism is younger than early Late Cretaceous orogenic events and contemporaneous with formation of the collapse-type Srednogorie sedimentary basin. Three volcanic intercalations within the oldest sedimentary succession of the Srednogorie zone exposed along the Tolponitsa river show  $^{40}\text{Ar}/^{39}\text{Ar}$  ages between 93 and 89 Ma and at ca. 86 Ma. Biotites from the Elshitsa granodiorite give an age of 86 Ma. Muscovite from an alteration zone at Elshitsa yield an age of 88 Ma. Amphiboles from a dacite porphyry from Vlaykov Vruh yield an age at 80 Ma. Biotites from the Velichkovo granodiorite give ages at 78–80 Ma.

Amphibole ages in part date hydrothermal alteration as the ages are clearly similar to U-Pb zircon ages from the same plutons, i.e. subvolcanic intrusions. Together with previous  $^{40}\text{Ar}/^{39}\text{Ar}$  amphibole and mica and numerous U-Pb zircon ages from mainly Late Cretaceous plutonic rocks of the Srednogorie area, the new ages display the following major trends: Magmatism lasted over a long period ranging from ca. 93 to 78 Ma. Both the plutonic and volcanic successions yield similar age groups, which are: 93–89 Ma, 86–84 Ma and 80–78 Ma. The age groups and their distribution show that magmatism was discontinuous and shifted southwards. Older subvolcanic rocks (93–89 Ma) developed in a regime of ca. N–S extension. They show that the southward prograding magmatism is older than dextral shearing, which developed between 86–78 Ma within ca. N–S compressional tectonic conditions. The geodynamic setting of the late Cretaceous magmatism in the Srednogorie zone is still controversial. The relationships within the Panagyurishte region, specifically the early stage of extension combined with calc-alkaline magmatism, could be explained by either retreat of a subduction zone or by slab break-off. The subsequent compressional phase is likely related to intra-orogenic shortening following collision.

## ZUSAMMENFASSUNG

$^{40}\text{Ar}/^{39}\text{Ar}$  Alter wurden bestimmt für Amphibole und Glimmer aus spätkreuzischen plutonischen und vulkanischen Abfolgen der Panagyurishte Region (Bulgarien), die Teil des kalkkalischen bis alkalischen Banatgürtels ist, der sich von den Apuseni Bergen bis zum Schwarzen Meer erstreckt und Weltklasse Cu-Au-Lagerstätten enthält. Der Magmatismus war aktiv nach der Kollision und den orogenen Ereignissen in der frühen Oberkreide und gleichzeitig zur Entstehung des Srednogorie Sedimentbeckens vom Kolapstyp. Drei vulkanische Einschaltungen in den ältesten Sedimentabfolgen der Srednogorie Zone, die entlang des Flusses Tolponitsa aufgeschlossen sind, zeigen  $^{40}\text{Ar}/^{39}\text{Ar}$  Alter zwischen 93 und 89 Ma, sowie ca. 86 Ma. Biotite aus dem Elshitsa-Granodiorit ergeben ein Alter von 86 Ma. Muskovite aus einer Alterationszone in Elshitsa ergeben ein Alter von 88 Ma. Amphibole eines Dazitporphyrs von Vlaykov Vruh ergeben ein Alter von 80 Ma. Biotite des Velichkovo-Granodiorits ergeben Alter von 78–80 Ma.

Die Amphibolalter datieren teilweise die hydrothermale Alteration, da die Alter ähnlich den U-Pb Zirkonaltern aus denselben Plutonen (subvulkanische Intrusionen) sind. Zusammen mit früheren  $^{40}\text{Ar}/^{39}\text{Ar}$  Amphibol- und Glimmeraltern sowie zahlreichen U-Pb Zirkonaltern von spätkreuzischen, plutonischen Gesteinen des Srednogorie-Gebietes, zeigen die neuen Daten folgende Haupttrends: Der Magmatismus hielt über eine längere Zeit zwischen 93 und 78 Ma an. Die plutonischen und vulkanischen Abfolgen zeigen ähnliche Altersgruppen: 93–89 Ma, 86–84 Ma und 80–78 Ma. Die Altersgruppen zeigen durch ihre Verteilung, dass der Magmatismus unterbrochen war und nach Süden wanderte. Die älteren subvulkanischen Gesteine (93–89 Ma) entstanden in einem N–S gerichteten Extensionsregime. Sie zeigen, dass der nach Süden fortschreitende Magmatismus älter ist als die dextrale Scherbewegung, welche zwischen 86 und 78 Ma unter N–S gerichteter Kompression entstanden war. Die Geodynamik des spätkreuzischen Magmatismus in der Srednogorie Zone wird immer noch kontrovers diskutiert. Die Beziehung der Panagyurishte-Region, vor allem das frühe Extensions-Stadium mit kalkkalinem Magmatismus, kann durch einen Rückzug der Subduktionszone oder Abreissen der subduzierten Lithosphäre erklärt werden. Die folgende Kompressionsphase dürfte auf die intra-orogene Kürzung in Folge der Kollision zurückzuführen sein.

## Introduction

The nature and evolution of the Banatite belt (von Cotta 1864; Berza et al. 1998; Ciobanu et al. 2002; von Quadt et al. 2005) also referred to as Banat-Srednogorie belt is still enigmatic. It

consists of Upper Cretaceous volcanic, subvolcanic and shallow plutonic rocks in southeastern Europe with widespread ore mineralizations (Berza et al. 1998; Heinrich & Neubauer 2002). The Banat-Srednogorie belt extends from the Black Sea through the Bulgarian Srednogorie zone and the Serbian

<sup>1</sup> Division of General Geology and Geodynamics, University of Salzburg, Hellbrunner Str. 34, A-5020 Salzburg, Austria

<sup>2</sup> Department of Geology, Sofia University, Tzar Osvoboditel Blv. 15, Sofia 1000, Bulgaria

\*Corresponding author; present address: Nagra, Hardstrasse 73, 5430 Wettingen, Switzerland. E-mail: andrea.rieser@nagra.ch

Timok-Majdanpek area to the Romanian Apuseni Mountains (Fig. 1) and possibly to the Western Carpathians. It is known among various terms including Apuseni-Timok-Srednogorie Magmatic and Mineralization belt (e.g. Jankovic 1997; Berza et al. 1998; Ciobanu et al. 2002). Although much work is done because of its high economic importance of Cu-Au and other mineralizations the tectonic evolution of the Banat-Srednogorie belt is not yet fully understood (e.g. Berza et al. 1998; Ciobanu et al. 2002; Neubauer 2002; von Quadt et al. 2002, 2005). Particularly no work has been done on correlating widespread volcanic rocks and areally separated plutonic centres. We present new  $^{40}\text{Ar}/^{39}\text{Ar}$  mineral ages from plutonic and volcanic rocks and some alteration minerals from the Panagyurishte region with the main emphasis to reveal the age variation of magmatism, the correlation of plutonic suites with their possible volcanic products as well as the possible timing of hydrothermal overprint. The new data may help to elucidate aspects of the tectonic evolution of the Panagyurishte region in Bulgaria, where a NNW-trending zone of Late Cretaceous calc-alkaline magmatic rocks formed across the principal E-W striking zone.

### Geological setting

The principal Cretaceous structures of the Alpine-Balkan-Carpathian-Dinaride (ABCD) orogen are that of a thick-skinned

orogenic wedge, which formed in response to collision of continental microplates (e.g. Channell & Kozur 1997; Ricou et al. 1998; Stampfli & Mosar 1999; Neugebauer et al. 2001; Neubauer 2002; Csontos & Vörös 2004). The principal Late Jurassic to Cretaceous orogenic structures are common features for the whole internal Cretaceous ABCD belt, particularly the Eastern Alps, Carpathians and Apuseni Mountains. As it is now well established, we can distinguish between (1) Late Jurassic obduction of oceanic crust in Dinaric, Vardar, Mures and Meliata ophiolite belts, (2) Early to early Late Cretaceous collisional structures, mainly ductile thrusts, (3) Late Cretaceous formation of collapse sedimentary basins, which are in southeast sectors associated with calc-alkaline magmatic rocks, and ductile low-angle normal and high-angle strike-slip faults, which relate to basin formation (Burg et al. 1990; Ricou et al. 1998; Willingshofer et al. 1999).

The Bulgarian Balkan region is linked by the Serbian Timok zone with the extension of the Southern Carpathians surrounding the western Moesian platform. In Bulgaria, the zone with specific Late Cretaceous sedimentary/volcanogenic basins is called Srednogorie zone (Aiello et al. 1977; Boccaletti et al. 1974, 1978; Popov 1987; Nachev 1993; Popov & Popov 1997, 2000; Ciobanu et al., 2002). The Srednogorie zone extends to the Black Sea and is also superposed onto the southerly adjacent Strandja zone (with mainly Late Jurassic tectonism; Okay et al. 2001). The central Srednogorie zone (Fig. 2) comprises a pre-Alpine basement of the Balkanide type (e.g. Arnaudov et al. 1989), an upper Carboniferous to Triassic cover succession and, above a pronounced angular unconformity, the Srednogorie Group (e.g. Karagjuleva et al. 1974; Foose & Manheim 1975; Aiello et al. 1977; Popov & Popov 2000). The stratigraphic range of the Srednogorie Group is from Turonian (Stoykov & Pavlishina 2003) to Maastrichtian (Moev & Antonov 1978; Popov & Popov 2000). The basin fill mainly comprises clastic terrigenous sequences with subordinate pelagic marls, shales, turbidites, and three levels of volcanic intercalations (Aiello et al. 1977; Popov & Popov 2000), particularly along the Tolponitsa section. The lowermost volcanic succession within the Srednogorie Group is exposed at Chelopech and is determined as Turonian in age by means of pollen in the Vozdol Sandstone (Stoykov & Pavlishina 2003).

The basement of the Srednogorie zone experienced amphibolite-grade late Variscan and weak early Late Cretaceous metamorphism and associated ductile deformation between 105 and 99 Ma (Velichkova et al. 2004). The southward increasing, weak metamorphic overprint also affected the Late Palaeozoic-Triassic to Albian cover (Minkovska et al. 2002) and was associated with ductile top-W shear due to transport of the tectonic overburden. The metamorphic overprint reached very low- to low-grade conditions and is dated at 102 to 100 Ma by the  $^{40}\text{Ar}/^{39}\text{Ar}$  method (Velichkova et al. 2004). After a short period of erosion and denudation, the Srednogorie volcanosedimentary basin was formed, which is associated with calc-alkaline and subordinate alkaline volcanic and some subvolcanic and plutonic rocks. These are partly rich in ore mineralizations

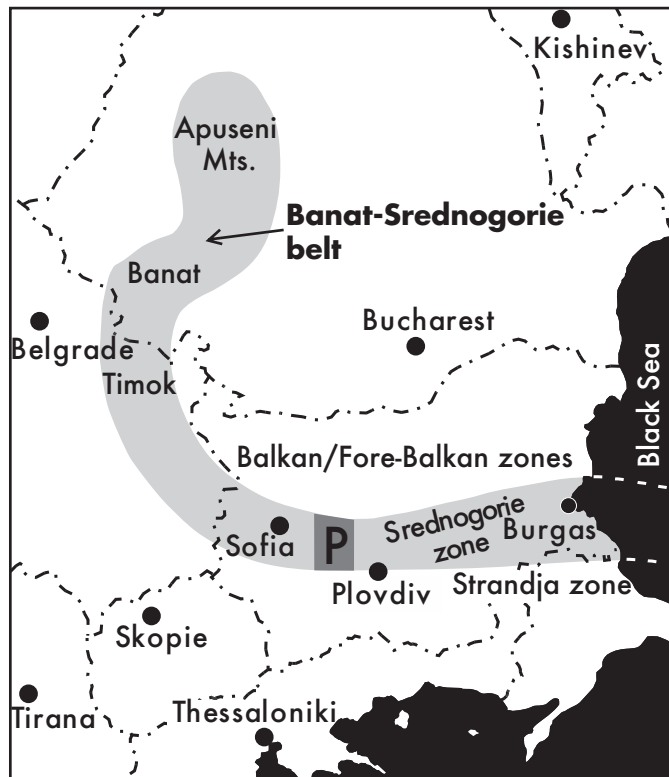


Fig. 1. Overview map of southeastern Europe displaying the U-shaped Banat-Srednogorie belt. P – Panagyurishte corridor (modified from Handler et al. 2004).

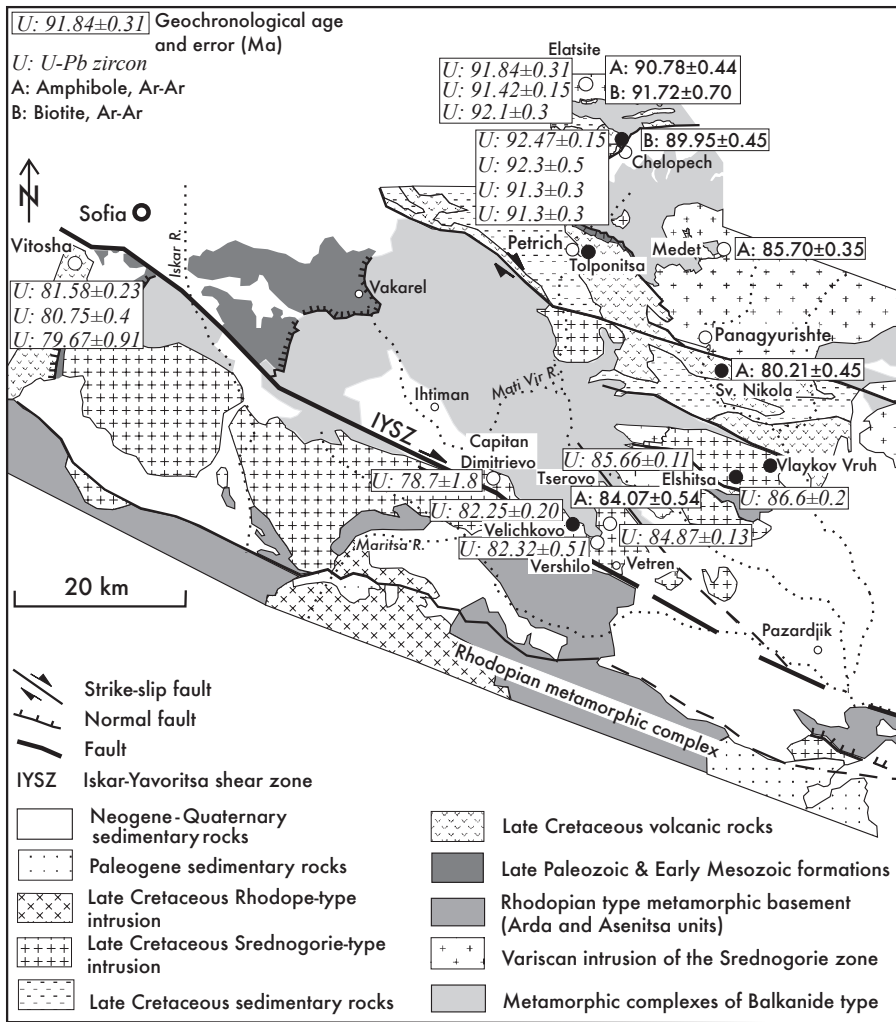


Fig. 2. Simplified tectonic map of Central Srednogorie and the northern margin of the Rhodope massif displaying sample locations (bold numbers; modified after Handler et al. 2004). Ages from von Quadt et al. (2005; U-Pb) and Lips et al. (2004;  $^{40}\text{Ar}/^{39}\text{Ar}$ ).

(Aiello et al. 1977; Berza et al. 1998; Boccaletti et al. 1974, 1978; Popov & Popov 2000; von Quadt et al. 2005).

Because of the calc-alkaline magmatism, the Srednogorie zone is interpreted to represent an intra-arc basin (e.g. Aiello et al. 1977) or post-collisional successor-type, respectively rift basin (e.g. Popov 1987; Popov & Popov 2000).

Upper Cretaceous high-level plutonic suites, here collectively referred to as “Banatites”, and some subordinate volcanic sequences (von Cotta 1864) extend from the northern Apuseni Mountains in Romania to the Black Sea. Many different terms have been proposed for this belt but for simplicity we here use Banatite belt. These Banatites are associated with various types of mineralization including porphyry copper and replacement ores (Popov 1987, 1996; Berza et al. 1998; Popov & Popov 2000, Ciobanu et al. 2002; von Quadt et al. 2005). Generally calc-alkaline suites largely predominate, although minor alkaline rocks were reported from the Bulgarian Srednogorie zone (e.g. Boccaletti et al. 1974, 1978; Berza et al. 1998 and references therein). The Panagyurishte region is a specific, ca. NNW trend-

ing zone across the generally E–W striking Banatite belt in Bulgaria with predominantly shallow intrusive bodies, mainly porphyries and associated porphyry Cu-Au and epithermal Cu-Au mineralizations (Strashimirov & Popov 2000; Moritz et al. 2004; von Quadt et al. 2005).

K-Ar ages from volcanic and plutonic rocks ranging from ca. 90 to 65 Ma have been reported by Lilov & Stanisheva-Vassileva (1998) and Lilov & Chipchakova (1999). These were recently compiled by von Quadt et al. (2005). Recent U-Pb zircon and  $^{40}\text{Ar}/^{39}\text{Ar}$  mineral data from Late Cretaceous volcanic and plutonic rocks and of alteration products exposed in the Panagyurishte region are compiled in Table 1. Peytcheva et al. (2001), von Quadt et al. (2002, 2003), Chambefort et al. (2003), Stoykov et al. (2004), Peytcheva et al. (2003) and von Quadt et al. (2005) reported U-Pb zircon ages from several plutons ranging between ca. 92 and 78 Ma.  $^{40}\text{Ar}/^{39}\text{Ar}$  mineral dating gave similar results (Handler et al. 2004), with ages ranging also between 92 and 78 Ma (Table 1). Recently, Lips et al. (2004) reported some  $^{40}\text{Ar}/^{39}\text{Ar}$  ages from plutonic host rocks

Table 1. Geochronological data for the Central Srednogorie zone.

Locality	Rock type	Method	Age and error (Ma)	Reference
Elatsite	Quartz monzonite porphyry	U-Pb zircon	92.10 ± 0.30	von Quadt et al. (2002)
Elatsite	Diorite porphyry	U-Pb zircon	91.84 ± 0.31	von Quadt et al. (2002)
Elatsite	Granodiorite porphyry	U-Pb zircon	91.42 ± 0.15	von Quadt et al. (2002)
Elatsite	Monzonite dyke	$^{40}\text{Ar}/^{39}\text{Ar}$ amphibole	90.78 ± 0.44	Handler et al. (2004)
		$^{40}\text{Ar}/^{39}\text{Ar}$ biotite	91.72 ± 0.70	
Elatsite	Monzonite dyke	$^{40}\text{Ar}/^{39}\text{Ar}$ amphibole	91.20 ± 0.60	Lips et al. (2004)
Elatsite	Alteration white mica	$^{40}\text{Ar}/^{39}\text{Ar}$ white mica	79.40 ± 0.70	Lips et al. (2004)
Chelopech	Andesite	U-Pb zircon	91.47 ± 0.15	Chambefort et al. (2003)
Chelopech	Andesite I phase	U-Pb zircon	92.30 ± 0.50	Stoykov et al. (2004)
Chelopech	Trachydacite II phase	U-Pb zircon	91.30 ± 0.30	Stoykov et al. (2004)
Chelopech	Andesite III phase	U-Pb zircon	91.30 ± 0.30	Stoykov et al. (2004)
Chelopech	Andesite	Ar-Ar biotite	89.95 ± 0.45	Handler et al. (2004)
Chelopech	Subvolcanic andesite	U-Pb zircon	92.22 ± 0.30	Stoykov et al. (2004)
Chelopech	Andesitic breccia	U-Pb zircon	91.45 ± 0.15	Moritz et al. (2004)
Medet	Granodiorite	$^{40}\text{Ar}/^{39}\text{Ar}$ amphibole	85.70 ± 0.35	Handler et al. (2004)
Medet	Monzodiorite	$^{40}\text{Ar}/^{39}\text{Ar}$ biotite	90.40 ± 0.90	Lips et al. (2004)
Medet	Monzodiorite	$^{40}\text{Ar}/^{39}\text{Ar}$ alteration	79.00 ± 0.80	Lips et al. (2004)
		white mica	79.40 ± 0.70	
			79.50 ± 0.70	
Medet	Quartz-monzodiorite	U-Pb zircon	89.61 ± 0.26	von Quadt et al. (2005)
Elshitsa	Granite	U-Pb zircon	86.60 ± 0.10	Peytcheva et al. (2003)
Elshitsa	Subvolcanic dacite	U-Pb zircon	86.11 ± 0.23	Peytcheva et al. (2003)
Elshitsa	Granodiorite	$^{40}\text{Ar}/^{39}\text{Ar}$ amphibole	84.07 ± 0.54	Handler et al. (2004)
Vlaykov Vruh	Hydrothermal rutile	U-Pb rutile	85.66 ± 0.11	Peytcheva et al. (2003)
Sv. Nikola	Andesite	$^{40}\text{Ar}/^{39}\text{Ar}$ amphibole	80.21 ± 0.45	Handler et al. (2004)
Velichkovo	Granodiorite	U-Pb zircon	84.60 ± 0.30	Peytcheva & von Quadt (2003)
Velichkovo	Gabbro	U-Pb zircon	82.16 ± 0.10	Peytcheva & von Quadt (2003)
Vetren	Hybrid gabbro	U-Pb zircon	84.87 ± 0.13	Peytcheva & von Quadt (2003)
Vershilo	Granite	U-Pb zircon	82.25 ± 0.20	Peytcheva et al. (2001)
Capitan Dimitriev	Monzodiorite (hybrid gabbro)	U-Pb zircon	78.60 ± 0.30	Kamenov et al. (2002)
Vitosha	Andesite	U-Pb zircon	80.75 ± 0.40	Atanassova-Vladimirova (2004)
Vitosha	Syenite	U-Pb zircon	79.67 ± 0.91	Atanassova-Vladimirova (2004)
Vitosha	Gabbro	U-Pb zircon	81.58 ± 0.23	Atanassova-Vladimirova (2004)

of Elatsite and Medet deposits, which are in the range of the before mentioned ages. Sericite from hydrothermal alteration zones of these two deposits, however, gave consistent ages of around 80 Ma. The various authors interpreted their ages to record a single stage of hydrothermal activity and mineralization, consistent with similar ages in the Serbian Bor and Majdanpek regions. This view contrasts with U-Pb zircon dating in the Elatsite deposit, from which von Quadt et al. (2002) reported an age of 92–91 Ma, based on dating of pre- and post-mineralization dykes.

The WNW-striking steep Maritsa fault separates the Srednogorie zone from the southerly adjacent Rhodope massif. The Maritsa fault also includes in part sheared Upper Cretaceous granites, which intruded between 84 and 78 Ma (von Quadt et al. 2002, 2003, 2005). In the Rhodope massif, the uppermost unit is a Cretaceous metamorphic unit, which formed within amphibolite facies conditions (e.g. Burg et al. 1990, 1993; Ricou et al., 1998). Furthermore, the data suggest that the Maritsa shear zone and its splays to the north (e.g. Iskar-Yavoritsa, Kameni-

tsa-Rakovitsa fault zones etc.) can be regarded together as a Cretaceous wrench corridor, which was active under greenschist facies metamorphic conditions. The zone is intruded by Upper Cretaceous granites and diorites, which are partly affected by ductile shearing. The age of intrusions varies between 84 and 78 Ma (von Quadt et al. 2002, 2005) and represents therefore the minimum duration of dextral shearing. The age sequence suggests a continuous or stepwise exhumation and surface uplift contemporaneous with the subsidence in the Srednogorie basin (Burg et al. 1990; Ricou et al. 1998). This matches the observation of a southerly located hinterland of clastic successions in the Srednogorie basin (Aiello et al. 1977), which can be identified as the Rhodope massif.

#### $^{40}\text{Ar}/^{39}\text{Ar}$ analytical techniques

Preparation of the samples before and after irradiation, the  $^{40}\text{Ar}/^{39}\text{Ar}$  analyses and age calculations were carried out at the ARGONAUT Laboratory at the University of Salzburg (Liu et

al. 2001; Handler et al. 2004). Mineral concentrates are packed in aluminium-foil and loaded in quartz vials. For calculation of the J-values, flux-monitors are placed between every 4–5 unknown samples, which yields a distance of ca. 5 mm between adjacent flux-monitors. The sealed quartz vials were irradiated in the MTA KFKI reactor (Debrecen, Hungary) for 16 hours. Correction factors for interfering isotopes have been calculated from 10 analyses of two Ca-glass samples and 22 analyses of two pure K-glass samples, and are:  $^{36}\text{Ar}/^{37}\text{Ar}_{(\text{Ca})} = 0.00026025$ ,  $^{39}\text{Ar}/^{37}\text{Ar}_{(\text{Ca})} = 0.00065014$ , and  $^{40}\text{Ar}/^{39}\text{Ar}_{(\text{K})} = 0.015466$ . Variations in the neutron-flux were monitored with DRA1 sanidine standard for which a  $^{40}\text{Ar}/^{39}\text{Ar}$  plateau age of  $25.03 \pm 0.05$  Ma has been reported (Wijbrans, oral communication, 1998). This age represents an update of the value reported in Wijbrans et al. (1995). DRA1 was intercalibrated with an age of 27.92 Ma from the TCR sanidine (Wijbrans et al. 1995) for which Renne et al. (1998) reported an age of 28.34 Ma. However, recent intercalibrations seem to yield again a slightly younger age. So, we use the above-mentioned age of  $25.03 \pm 0.05$  Ma until the new calibrations are available.

After irradiation the minerals were unpacked from the quartz vials and the aluminium-foil packets and handpicked into 1 mm diameter holes within one-way Al-sample holders.  $^{40}\text{Ar}/^{39}\text{Ar}$  analyses are carried out using a UHV Ar-extraction line equipped with a combined MERCHANTEK™ UV/IR laser ablation facility and a VG-ISOTECH™ NG3600 Mass Spectrometer. Stepwise heating analyses of samples are performed using a defocused (~1.5 mm diameter) 25 W CO<sub>2</sub>-IR laser operating in Tem<sub>00</sub> mode at wavelengths between 10.57 and 10.63 μm. The laser is controlled from a PC and the position of the laser on the sample is monitored through a double-vacuum window on the sample chamber via a video camera in the optical axis of the laser beam on the computer screen. Gas clean-up is performed using one hot and one cold Zr-Al SAES getter. Gas admittance and pumping of the mass spectrometer and the Ar-extraction line are computer controlled using pneumatic valves. The NG3600 is a 18 cm radius 60° extended geometry instrument, equipped with a bright Nier-type source operated at 4.5 kV. Measurement is performed on an axial electron multiplier in static mode, peak-jumping and stability of the magnet is controlled by a Hall-probe. For each increment the intensities of  $^{36}\text{Ar}$ ,  $^{37}\text{Ar}$ ,  $^{38}\text{Ar}$ ,  $^{39}\text{Ar}$  and  $^{40}\text{Ar}$  are measured, the baseline readings on mass 35.5 are automatically subtracted. Peak intensities are back-extrapolated over 16 measured intensities to the time of gas admittance either by a straight line or a curved fit. Intensities are corrected for system blanks, background, post-irradiation decay of  $^{37}\text{Ar}$  and interfering isotopes. Isotopic ratios, ages and errors for individual steps are calculated following suggestions by McDougall & Harrison (1999) using decay factors reported by Steiger & Jäger (1977). Definition and calculation of plateau ages has been carried out using ISOPLOT/EX (Ludwig 2001). We use the new time calibration of Gradstein et al. (2004).

#### **$^{40}\text{Ar}/^{39}\text{Ar}$ dating results**

For this study we selected samples from six locations in the Panagyurishte zone (Fig. 2). Samples were carefully selected to avoid possible effects of post-volcanic/post-plutonic alteration. However, we realised during analytical work that several samples show some variable degree of secondary alteration (see below). A few biotite and amphibole grains display variable but minor and clearly recognizable alteration in thin sections. This observation suggests a weak post-magmatic thermal overprint, possibly due to a very low-grade thermal event. Some biotite concentrates indeed show low-temperature overprint in low-energy steps of the experiment. Some important details of petrography influencing the interpretation are shown in Figure 3 and described in the main text. Petrographic details of all dated samples are given in the Appendix.  $^{40}\text{Ar}/^{39}\text{Ar}$ -dating results are presented in Table 2 and are graphically shown in Figures 4–8.

#### *Chelopech*

An experiment was performed on an amphibole concentrate from sample BULG-42, an andesite from the Vosdol valley NE of Chelopech. Note that some amphiboles are slightly altered in thin section (Fig. 3a) and that some argon might have been lost. The first three steps comprising 4.5 percent of  $^{39}\text{Ar}$  released yielded extraneous argon. Steps 3–11 yielded a plateau age of  $86.53 \pm 0.54$  Ma constituting together 95.5 percent of  $^{39}\text{Ar}$  released (Fig. 4). This age is younger than the biotite age ( $89.95 \pm 0.45$  Ma) reported from the same locality by Handler et al. (2004) and the U-Pb age of  $91.3 \pm 0.3$  by Stoykov et al. (2004). However, the plateau age demonstrates that most sectors within the amphibole from which argon was released during the experiment are in equilibrium. Therefore we suggest that the age rather indicates hydrothermal alteration, which opened the argon isotopic system within the amphibole.

#### *Volcanic rocks from the Tolponitsa section*

$^{40}\text{Ar}/^{39}\text{Ar}$  release spectra for all Tolponitsa samples are shown in Figure 5. An experiment was performed on amphibole (BULG-63) from a massive lava flow from the base of the section, which is underlain by Turonian sandstones. The first step comprising 12.1 percent of  $^{39}\text{Ar}$  released yielded extraneous argon. Steps 2–11 yielded a plateau age of  $97.77 \pm 0.68$  Ma constituting together 79.2 percent of  $^{39}\text{Ar}$  released (Fig. 5a). This age represents the maximum age of cooling through ca. 500 °C. Note, that the true age could be slightly younger, because of the presence of extraneous argon.

Sample BULG-64 is a coarse-grained biotite–andesite tuff (?) from the intermediate volcanic level, underlain by Upper Turonian limestones. It comprises mm-sized well preserved amphiboles (Fig. 3b). The first step yielded extraneous argon. Steps 6–13 yielded a plateau age of  $90.60 \pm 0.51$  Ma for the amphiboles constituting together 94.3 percent of  $^{39}\text{Ar}$  released (Fig. 5b). This age represents the maximum age of cooling

Table 2.  $^{40}\text{Ar}/^{39}\text{Ar}$  results from stepwise heating analyses of amphibole and mica from magmatic rocks from the Central Srednogorie zone.

Step	<b>BULG 42</b>		<b>J-value: <math>0.01842 \pm 0.0018</math></b>		<b>amphibole</b>	<b>Chelopech</b>				<b>age [Ma]</b>	<b>±</b>
	$^{36}\text{Ar}/^{39}\text{Ar}^a$	$\pm$	$^{37}\text{Ar}/^{39}\text{Ar}^b$	$\pm$	$^{40}\text{Ar}/^{39}\text{Ar}^a$	$\pm$	% $^{40}\text{Ar}^c$	% $^{39}\text{Ar}$			
1	0.656727	0.016341	49.504097	0.010762	213.611	6.020	9.2	0.1	663.14	138.63	
2	0.475562	0.008735	57.335921	0.006397	153.672	3.013	8.6	0.2	522.01	75.11	
3	0.014522	0.000313	8.709697	0.000327	7.236	0.093	40.7	4.2	116.45	3.10	
4	0.002264	0.000064	6.007759	0.000062	2.838	0.019	76.4	24.5	85.21	1.03	
5	0.002893	0.000088	5.452209	0.000090	3.095	0.026	72.4	18.6	86.08	1.18	
6	0.002121	0.000075	3.213338	0.000078	3.115	0.022	79.9	19.2	88.38	1.11	
7	0.004385	0.000689	10.762406	0.000620	3.230	0.204	59.9	2.3	89.66	6.50	
8	0.007965	0.001018	21.965959	0.000817	3.321	0.301	29.1	1.7	86.92	9.57	
9	0.003796	0.000225	11.344899	0.000192	2.951	0.066	62.0	7.3	87.76	2.27	
10	0.005057	0.000130	10.559726	0.000105	3.382	0.038	55.8	13.6	87.67	1.48	
11	0.004250	0.000196	13.065205	0.000170	2.938	0.058	57.3	8.4	87.39	2.02	
3–11							95.5		86.53		0.54
Step	<b>BULG 63</b>		<b>J-value: <math>0.01837 \pm 0.0001837</math></b>		<b>amphibole</b>	<b>Tolponitsa</b>				<b>age [Ma]</b>	<b>Step</b>
	$^{36}\text{Ar}/^{39}\text{Ar}^a$	$\pm$	$^{37}\text{Ar}/^{39}\text{Ar}^b$	$\pm$	$^{40}\text{Ar}/^{39}\text{Ar}^a$	$\pm$	% $^{40}\text{Ar}^c$	% $^{39}\text{Ar}$			
1	0.26415	0.00022	2.42710	0.00012	84.461	0.069	7.6	12.1	206.04	2.82	
2	0.01537	0.00009	2.97219	0.00010	7.291	0.028	37.7	16.0	95.72	1.27	
3	0.02670	0.00025	10.06128	0.00023	10.060	0.075	21.6	6.1	95.16	2.52	
4	0.04883	0.00047	16.69299	0.00048	16.325	0.140	11.6	3.0	102.98	4.50	
5	0.05371	0.00068	17.55904	0.00073	17.765	0.203	10.7	2.1	105.12	6.41	
6	0.03783	0.00090	20.26726	0.00099	12.803	0.265	12.7	1.5	103.37	8.36	
7	0.02987	0.00068	12.64301	0.00070	11.098	0.200	20.5	2.0	104.76	6.35	
8	0.01141	0.00055	8.85281	0.00065	5.751	0.164	41.4	2.0	98.71	5.22	
9	0.00538	0.00021	5.90957	0.00022	4.248	0.063	62.6	6.1	100.23	2.21	
10	0.00999	0.00036	12.86906	0.00042	5.055	0.106	41.6	3.4	100.05	3.46	
11	0.01273	0.00004	11.78550	0.00004	5.902	0.012	36.3	37.1	98.47	1.03	
12	0.01743	0.00087	23.15933	0.00116	6.798	0.258	24.2	1.2	111.35	8.12	
13	0.01578	0.00118	24.75800	0.00141	7.012	0.349	33.5	1.0	137.36	10.80	
14	0.01873	0.00041	12.21201	0.00034	7.645	0.120	27.6	3.6	98.64	3.89	
15	0.00953	0.00113	1.09423	0.00110	4.787	0.333	41.2	1.2	66.46	10.65	
16	0.00633	0.00084	2.16679	0.00075	4.282	0.247	56.3	1.7	83.06	7.86	
2–11							79.2		97.77		0.68
Step	<b>BULG 64</b>		<b>J-value: <math>0.01835 \pm 0.0001835</math></b>		<b>amphibole</b>	<b>Tolponitsa</b>				<b>age [Ma]</b>	<b>±</b>
	$^{36}\text{Ar}/^{39}\text{Ar}^a$	$\pm$	$^{37}\text{Ar}/^{39}\text{Ar}^b$	$\pm$	$^{40}\text{Ar}/^{39}\text{Ar}^a$	$\pm$	% $^{40}\text{Ar}^c$	% $^{39}\text{Ar}$			
1	0.50365	0.01025	106.42456	0.00940	159.594	3.499	6.7	0.2	572.24	84.48	
2	0.34638	0.00487	88.07571	0.00472	118.080	1.582	13.3	0.3	654.85	36.84	
3	0.23260	0.00660	91.38415	0.00742	78.779	2.062	12.8	0.2	518.31	51.42	
4	0.12225	0.00336	59.61451	0.00387	42.317	1.010	14.6	0.4	337.09	27.92	
5	0.00993	0.00711	13.01264	0.00926	11.083	2.106	73.5	0.1	281.80	59.69	
6	0.00485	0.00015	5.68808	0.00014	3.772	0.046	62.0	8.5	89.51	1.68	
7	0.00283	0.00006	6.28272	0.00007	3.219	0.018	74.0	17.8	92.36	1.07	
8	0.00270	0.00016	7.76503	0.00016	2.942	0.048	72.9	7.9	88.51	1.73	
9	0.00312	0.00007	7.81528	0.00007	3.149	0.020	70.7	18.4	91.22	1.08	
10	0.00363	0.00004	8.01508	0.00004	3.215	0.013	66.6	31.5	89.02	0.96	
11	0.00483	0.00036	13.09070	0.00040	3.296	0.106	56.7	3.1	93.08	3.45	
12	0.00881	0.00067	20.27155	0.00066	3.907	0.199	33.4	1.6	93.08	6.32	
13	0.00474	0.00019	13.19645	0.00020	3.236	0.057	56.7	5.6	92.27	2.00	
14	0.01239	0.00056	18.77763	0.00051	4.263	0.164	14.1	2.1	66.79	5.28	
15	0.00354	0.00062	9.35729	0.00063	4.895	0.184	78.6	1.9	145.61	5.78	
16	0.00748	0.00280	7.91103	0.00301	9.026	0.828	75.5	0.4	231.09	24.22	
3–16							94.3		90.60		0.51

Table 2. (Continued).

<b>BULG 104</b>		<b>J-value: <math>0.01824 \pm 0.0001824</math></b>		<b>amphibole</b>	<b>Tolponitsa</b>				<b>age [Ma]</b>	<b>±</b>
<b>Step</b>	<b><math>^{36}\text{Ar}/^{39}\text{Ar}^a</math></b>	<b>±</b>	<b><math>^{37}\text{Ar}/^{39}\text{Ar}^b</math></b>	<b>±</b>	<b><math>^{40}\text{Ar}/^{39}\text{Ar}^a</math></b>	<b>±</b>	<b>%<math>^{40}\text{Ar}^c</math></b>	<b>%<math>^{39}\text{Ar}</math></b>		
1	0.13500	0.00034	8.41113	0.00032	49.173	0.103	18.9	3.7	282.17	3.90
2	0.03390	0.00051	7.05959	0.00056	13.980	0.152	28.3	2.5	125.91	4.82
3	0.03705	0.00045	3.29817	0.00039	13.839	0.133	20.9	3.4	92.74	4.25
4	0.07180	0.00135	6.65374	0.00106	24.167	0.400	12.2	1.2	94.57	12.51
5	0.06441	0.00156	24.65833	0.00168	19.763	0.465	3.7	0.7	23.81	15.10
6	0.00704	0.00014	8.10366	0.00014	4.511	0.043	53.9	8.7	78.22	1.55
7	0.00563	0.00031	2.83516	0.00031	4.068	0.092	59.1	3.8	77.43	2.98
8	0.00301	0.00005	4.55444	0.00006	3.322	0.016	73.3	22.8	78.38	0.91
9	0.00433	0.00028	4.07598	0.00030	3.687	0.082	65.3	4.2	77.58	2.68
10	0.00314	0.00007	5.39738	0.00007	3.339	0.020	72.3	17.5	77.69	0.99
11	0.00605	0.00031	6.42112	0.00030	4.205	0.090	57.5	3.9	77.88	2.95
12	0.00451	0.00011	6.12214	0.00011	3.765	0.031	64.6	11.4	78.30	1.25
13	0.00493	0.00012	5.03330	0.00011	3.803	0.034	61.7	10.9	75.58	1.31
14	0.00507	0.00026	8.72435	0.00030	3.969	0.078	62.3	3.9	79.55	2.59
15	0.02382	0.00101	30.65219	0.00113	7.280	0.298	3.3	1.0	7.95	9.77
16	0.03378	0.00236	28.93469	0.00238	16.808	0.700	40.6	0.5	211.67	20.59
6–14							87.1		77.79	0.48
<b>BULG 105</b>		<b>J-value: <math>0.01823 \pm 0.0001823</math></b>		<b>amphibole</b>	<b>Tolponitsa</b>				<b>age [Ma]</b>	<b>±</b>
<b>Step</b>	<b><math>^{36}\text{Ar}/^{39}\text{Ar}^a</math></b>	<b>±</b>	<b><math>^{37}\text{Ar}/^{39}\text{Ar}^b</math></b>	<b>±</b>	<b><math>^{40}\text{Ar}/^{39}\text{Ar}^a</math></b>	<b>±</b>	<b>%<math>^{40}\text{Ar}^c</math></b>	<b>%<math>^{39}\text{Ar}</math></b>		
1	1.05460	0.00799	25.47703	0.00456	358.215	3.260	13.0	0.2	1157.45	57.08
2	0.14065	0.00383	22.53483	0.00423	65.974	1.190	37.0	0.3	711.43	27.04
3	0.33419	0.01019	140.89059	0.01089	111.955	3.327	11.8	0.1	709.80	74.07
4	0.31030	0.01673	89.99451	0.01506	120.149	5.581	23.7	0.1	940.97	109.20
5	0.16769	0.01111	89.50702	0.00811	74.710	3.417	33.7	0.1	870.25	69.71
6	0.21034	0.01386	146.84534	0.01213	72.556	4.320	14.3	0.1	653.99	99.02
7	0.00471	0.00037	1.42887	0.00034	1.870	0.109	25.6	3.1	18.75	3.57
8	0.00711	0.00075	12.04601	0.00064	2.371	0.223	11.4	1.6	38.75	7.19
9	0.00453	0.00056	0.08160	0.00050	3.567	0.165	62.5	2.0	71.58	5.28
10	0.00377	0.00024	1.66599	0.00021	3.625	0.072	69.3	4.8	84.43	2.41
11	0.00242	0.00005	5.99219	0.00005	2.876	0.016	75.1	23.6	84.03	0.96
12	0.00358	0.00004	7.73549	0.00004	3.121	0.012	66.1	29.1	85.32	0.92
13	0.00404	0.00005	8.01807	0.00005	3.135	0.015	62.0	24.5	82.19	0.93
14	0.00585	0.00012	8.58246	0.00011	3.706	0.035	53.4	9.1	84.72	1.38
15	0.00763	0.00097	5.67121	0.00089	3.865	0.285	41.7	1.1	65.83	9.08
10–14							91.2		83.99	0.49
<b>BULG 68</b>		<b>J-value: <math>0.01819 \pm 0.0001819</math></b>		<b>white mica</b>	<b>Tolponitsa</b>				<b>age [Ma]</b>	<b>±</b>
<b>Step</b>	<b><math>^{36}\text{Ar}/^{39}\text{Ar}^a</math></b>	<b>±</b>	<b><math>^{37}\text{Ar}/^{39}\text{Ar}^b</math></b>	<b>±</b>	<b><math>^{40}\text{Ar}/^{39}\text{Ar}^a</math></b>	<b>±</b>	<b>%<math>^{40}\text{Ar}^c</math></b>	<b>%<math>^{39}\text{Ar}</math></b>		
1	0.009137	0.000346	2.077009	0.000330	12.110	0.102	77.7	2.5	289.4	3.9
2	0.001520	0.000066	0.706527	0.000059	10.907	0.020	95.9	12.9	315.4	2.9
3	0.003437	0.000337	2.116231	0.000391	11.369	0.100	91.1	2.1	315.8	4.0
4	0.001187	0.000057	1.682124	0.000061	10.715	0.017	96.7	13.3	315.0	2.9
5	0.004310	0.000264	5.963758	0.000255	11.058	0.078	88.5	2.9	308.9	3.6
6	0.001711	0.000080	2.593962	0.000067	10.580	0.024	95.2	10.4	309.1	2.9
7	0.000213	0.000023	0.078313	0.000019	10.521	0.007	99.4	37.6	313.9	2.9
8	0.000000	0.000082	1.667125	0.000079	10.097	0.024	100.0	9.2	307.6	2.9
9	0.001327	0.000122	1.849361	0.000120	10.786	0.036	96.4	6.7	316.2	3.1
10	0.002712	0.000585	3.017928	0.000483	11.330	0.173	92.9	1.3	322.6	5.6
11	0.002966	0.000764	1.020185	0.000802	13.140	0.226	93.3	0.9	365.2	6.9
							96.6		313.0	1.1

Table 2. (Continued).

<b>BULG 102</b>		<b>J-value: <math>0.01822 \pm 0.0001822</math></b>		<b>amphibole</b>	<b>Sv. Nikola</b>		<b>%<sup>40</sup>Ar<sup>c</sup></b>	<b>%<sup>39</sup>Ar</b>	<b>age [Ma]</b>	<b>±</b>
<b>Step</b>	<b><sup>36</sup>Ar/<sup>39</sup>Ar<sup>a</sup></b>	<b>±</b>	<b><sup>37</sup>Ar/<sup>39</sup>Ar<sup>b</sup></b>	<b>±</b>	<b><sup>40</sup>Ar/<sup>39</sup>Ar<sup>a</sup></b>	<b>±</b>				
1	0.88922	0.00150	3.46449	0.00070	310.218	0.563	15.3	3.5	1130.35	12.97
2	0.93034	0.00373	26.38875	0.00225	316.580	1.427	13.2	1.1	1070.11	27.15
3	0.88765	0.00564	42.77263	0.00272	301.192	2.162	12.9	0.8	1050.59	40.49
4	0.75991	0.00634	60.22073	0.00355	246.383	2.285	8.9	0.7	733.26	50.39
5	0.53895	0.00487	29.40127	0.00368	194.486	1.761	18.1	0.7	953.08	34.93
6	0.28115	0.00191	15.00859	0.00152	98.337	0.600	15.5	1.7	475.66	15.73
7	0.07243	0.00047	8.84289	0.00041	25.943	0.139	17.5	7.0	164.36	4.47
8	0.01013	0.00305	39.09296	0.00350	6.389	0.903	53.2	0.7	203.52	26.60
9	0.00267	0.00008	7.29080	0.00008	3.011	0.024	73.8	27.6	89.14	1.14
10	0.00423	0.00030	5.96540	0.00024	3.559	0.088	64.8	8.9	88.57	2.90
11	0.01416	0.00113	22.32078	0.00103	5.120	0.333	18.3	2.2	85.89	10.48
12	0.00643	0.00054	9.66512	0.00044	3.859	0.160	50.8	5.0	86.81	5.08
13	0.00297	0.00009	6.49413	0.00008	3.048	0.028	71.2	27.5	85.50	1.20
14	0.00751	0.00098	9.02407	0.00083	4.238	0.290	47.6	2.6	87.04	9.14
15	0.00335	0.00025	8.49670	0.00022	3.166	0.073	68.7	9.6	90.69	2.45
16	0.03314	0.00545	31.23194	0.00492	10.605	1.612	7.7	0.4	104.31	50.01
9–16							83.8	87.77	0.75	
<b>BULG 84</b>		<b>J-value: <math>0.01831 \pm 0.0001821</math></b>		<b>amphibole</b>	<b>Vlaikov Vruh</b>		<b>%<sup>40</sup>Ar<sup>c</sup></b>	<b>%<sup>39</sup>Ar</b>	<b>age [Ma]</b>	<b>±</b>
<b>Step</b>	<b><sup>36</sup>Ar/<sup>39</sup>Ar<sup>a</sup></b>	<b>±</b>	<b><sup>37</sup>Ar/<sup>39</sup>Ar<sup>b</sup></b>	<b>±</b>	<b><sup>40</sup>Ar/<sup>39</sup>Ar<sup>a</sup></b>	<b>±</b>				
1	0.41241	0.01912	144.23093	0.01584	139.966	6.498	12.9	0.1	836.03	135.21
2	0.11499	0.00212	24.43853	0.00208	38.666	0.638	12.1	0.5	207.49	18.89
3	0.05658	0.00057	7.33744	0.00054	20.494	0.170	18.4	2.3	138.07	5.38
4	0.02571	0.00017	3.18666	0.00017	10.166	0.050	25.3	7.0	90.34	1.80
5	0.01605	0.00010	1.51789	0.00006	7.382	0.030	35.8	19.5	88.41	1.27
6	0.01829	0.00010	1.96562	0.00007	8.049	0.031	32.8	18.1	89.62	1.30
7	0.01148	0.00007	2.02866	0.00006	6.132	0.020	44.7	21.6	92.88	1.10
8	0.00492	0.00017	1.28867	0.00015	4.214	0.050	65.5	7.0	91.67	1.81
9	0.01041	0.00018	6.34758	0.00014	5.357	0.053	42.6	7.4	89.08	1.88
10	0.00673	0.00019	3.77320	0.00018	4.565	0.056	56.4	6.6	92.01	1.98
11	0.00857	0.00023	6.35752	0.00023	4.747	0.067	46.7	5.2	87.07	2.28
12	0.00399	0.00079	0.99845	0.00077	5.645	0.233	79.1	1.4	143.76	7.24
13	0.00968	0.00062	12.62547	0.00070	7.409	0.185	61.4	1.7	174.60	5.78
14	0.01701	0.00075	18.29393	0.00072	7.963	0.222	36.9	1.6	139.16	6.91
4–11							91.2	90.43	0.54	
<b>BULG 88</b>		<b>J-value: <math>0.01827 \pm 0.0001827</math></b>		<b>amphibole</b>	<b>Elshitsa</b>		<b>%<sup>40</sup>Ar<sup>c</sup></b>	<b>%<sup>39</sup>Ar</b>	<b>age [Ma]</b>	<b>±</b>
<b>Step</b>	<b><sup>36</sup>Ar/<sup>39</sup>Ar<sup>a</sup></b>	<b>±</b>	<b><sup>37</sup>Ar/<sup>39</sup>Ar<sup>b</sup></b>	<b>±</b>	<b><sup>40</sup>Ar/<sup>39</sup>Ar<sup>a</sup></b>	<b>±</b>				
1	0.01925	0.00124	1.29212	0.00134	18.444	0.368	69.2	1.4	380.48	10.42
2	0.03814	0.00191	6.51348	0.00156	21.962	0.568	48.7	1.1	336.53	15.83
3	0.03141	0.00134	1.28397	0.00130	14.076	0.398	34.1	1.3	154.10	12.13
4	0.03570	0.00129	7.49407	0.00120	11.314	0.383	6.8	1.4	43.42	12.32
5	0.01215	0.00056	8.19305	0.00053	6.784	0.165	47.1	3.2	121.95	5.22
6	0.01646	0.00040	19.75778	0.00039	7.502	0.119	35.2	4.2	133.24	3.87
7	0.00826	0.00011	11.95827	0.00010	4.404	0.031	44.6	16.8	92.82	1.34
8	0.00817	0.00010	12.60126	0.00009	4.401	0.031	45.1	21.0	95.12	1.33
9	0.00968	0.00055	15.94771	0.00055	4.788	0.162	40.2	3.1	101.59	5.15
10	0.00712	0.00014	14.22181	0.00014	3.986	0.042	47.2	12.8	95.92	1.62
11	0.01119	0.00026	13.36560	0.00021	5.239	0.076	36.9	8.1	95.36	2.56
12	0.01340	0.00037	14.30221	0.00029	5.788	0.109	31.6	5.8	94.43	3.52
13	0.00562	0.00021	12.86493	0.00020	3.698	0.063	55.1	9.7	97.43	2.19
14	0.00975	0.00063	23.00302	0.00062	5.226	0.186	44.9	2.9	132.20	5.84
15	0.00893	0.00032	18.82034	0.00028	4.513	0.094	41.5	6.4	107.11	3.10
16	0.03958	0.00211	32.50449	0.00197	14.759	0.626	20.8	0.9	177.75	18.78
7–13							77.2	94.98	0.71	

Table 2. (Continued).

	<b>BULG 88</b>	<b>J-value: <math>0.0182 \pm 0.000182</math></b>		<b>biotite</b>	<b>Elshitsa</b>			% <sup>40</sup> Ar <sup>c</sup>	% <sup>39</sup> Ar	age [Ma]	±
Step	<sup>36</sup> Ar/ <sup>39</sup> Ar <sup>a</sup>	±	<sup>37</sup> Ar/ <sup>39</sup> Ar <sup>b</sup>	±	<sup>40</sup> Ar/ <sup>39</sup> Ar <sup>a</sup>	±					
1	0.15205	0.00288	34.08011	0.00268	51.839	0.867	13.3	0.2	294.09	24.33	
2	0.02189	0.00059	8.10133	0.00057	10.002	0.173	35.3	0.8	131.76	5.44	
3	0.00802	0.00024	1.18137	0.00020	6.192	0.070	61.7	2.0	123.76	2.46	
4	0.01050	0.00108	7.81810	0.00111	6.241	0.320	50.3	0.4	118.91	9.90	
5	0.00740	0.00030	0.46290	0.00031	4.947	0.088	55.8	1.6	89.06	2.90	
6	0.00623	0.00030	0.82630	0.00028	4.477	0.088	58.9	1.7	86.10	2.88	
7	0.00326	0.00016	0.10891	0.00016	3.716	0.047	74.0	2.8	87.94	1.70	
8	0.00301	0.00009	0.01015	0.00007	3.580	0.026	75.2	5.1	85.82	1.17	
9	0.00180	0.00003	0.04461	0.00004	3.267	0.010	83.7	11.8	87.26	0.91	
10	0.00103	0.00009	0.86892	0.00010	2.932	0.026	89.7	4.6	85.96	1.17	
11	0.00052	0.00006	0.12482	0.00005	2.923	0.016	94.8	8.6	88.59	1.00	
12	0.00046	0.00006	0.03588	0.00006	2.922	0.018	95.4	7.0	88.87	1.04	
13	0.00073	0.00005	0.01489	0.00004	2.906	0.014	92.6	9.9	85.82	0.95	
14	0.00065	0.00007	1.64255	0.00006	2.860	0.020	93.3	6.4	89.09	1.06	
15	0.00097	0.00005	1.98408	0.00005	2.845	0.016	90.0	7.8	86.53	0.98	
16	0.00050	0.00008	0.05414	0.00007	2.815	0.023	94.7	5.3	85.13	1.11	
17	0.00075	0.00008	1.31207	0.00008	2.846	0.024	92.2	5.3	86.91	1.12	
18	0.00067	0.00007	0.53779	0.00006	2.834	0.021	93.1	5.9	85.41	1.06	
19	0.00138	0.00012	2.51846	0.00011	2.930	0.036	86.1	3.6	86.67	1.42	
20	0.00122	0.00009	2.17688	0.00008	2.867	0.025	87.4	4.7	85.38	1.15	
21	0.00001	0.00017	0.16592	0.00012	2.912	0.050	99.9	3.0	93.03	1.81	
22	0.00011	0.00030	1.62931	0.00025	3.020	0.089	98.9	1.5	98.99	2.93	
5–20								92.2	86.84	0.29	
	<b>BULG 89</b>	<b>J-value: <math>0.01819 \pm 0.0001819</math></b>		<b>white mica</b>	<b>Elshitsa</b>			% <sup>40</sup> Ar <sup>c</sup>	% <sup>39</sup> Ar	age [Ma]	±
Step	<sup>36</sup> Ar/ <sup>39</sup> Ar <sup>a</sup>	±	<sup>37</sup> Ar/ <sup>39</sup> Ar <sup>b</sup>	±	<sup>40</sup> Ar/ <sup>39</sup> Ar <sup>a</sup>	±					
1	0.00555	0.00026	0.00000	0.00023	5.452	0.077	69.9	2.4	120.99	2.64	
2	0.00544	0.00086	0.30886	0.00078	4.860	0.255	66.9	0.8	103.73	7.97	
3	0.00227	0.00010	1.52977	0.00010	3.713	0.028	82.0	6.6	97.19	1.29	
4	0.00098	0.00043	6.13942	0.00049	3.969	0.127	92.7	1.3	116.87	4.06	
5	0.00226	0.00004	0.37987	0.00003	3.526	0.011	81.1	18.9	91.48	0.95	
6	0.00179	0.00024	3.75722	0.00022	3.328	0.071	84.1	2.4	89.63	2.39	
7	0.00060	0.00008	1.26495	0.00007	3.099	0.024	94.3	7.0	93.40	1.18	
8	0.00126	0.00033	2.43221	0.00034	3.188	0.097	88.3	1.8	90.10	3.15	
9	0.00062	0.00006	0.60446	0.00007	3.028	0.018	93.9	8.9	91.01	1.06	
10	0.00094	0.00003	0.44540	0.00003	3.205	0.009	91.4	17.5	93.62	0.96	
11	0.00210	0.00017	2.03976	0.00017	3.403	0.050	81.8	3.4	89.13	1.78	
12	0.00131	0.00006	0.98383	0.00006	3.208	0.016	88.0	9.3	90.28	1.02	
13	0.00141	0.00025	4.23889	0.00024	3.273	0.073	87.3	2.6	91.42	2.44	
14	0.00029	0.00006	1.08150	0.00006	2.888	0.018	97.1	9.6	89.72	1.04	
15	0.00030	0.00016	1.72901	0.00018	2.957	0.047	97.0	3.4	91.72	1.73	
16	0.00135	0.00040	6.23004	0.00039	3.185	0.119	87.5	1.4	89.18	3.82	
17	0.00036	0.00022	2.44064	0.00021	2.922	0.065	96.4	2.7	90.15	2.20	
5–17								88.9	91.33	0.38	
	<b>BULG 101</b>	<b>J-value: <math>0.01825 \pm 0.0001825</math></b>		<b>amphibole</b>	<b>Elshitsa</b>			% <sup>40</sup> Ar <sup>c</sup>	% <sup>39</sup> Ar	age [Ma]	±
Step	<sup>36</sup> Ar/ <sup>39</sup> Ar <sup>a</sup>	±	<sup>37</sup> Ar/ <sup>39</sup> Ar <sup>b</sup>	±	<sup>40</sup> Ar/ <sup>39</sup> Ar <sup>a</sup>	±					
1	0.14649	0.00347	0.00000	0.00382	46.663	1.059	7.2	0.4	107.40	32.86	
2	0.07038	0.00180	0.00000	0.00199	24.386	0.536	14.7	0.9	113.98	16.59	
3	0.00893	0.00033	0.00000	0.00036	4.747	0.098	44.4	4.4	67.61	3.18	
4	0.00564	0.00013	0.00000	0.00014	3.583	0.039	53.4	11.6	61.47	1.38	
5	0.00493	0.00010	0.00000	0.00013	3.403	0.030	57.2	13.2	62.48	1.14	
6	0.00449	0.00007	0.00000	0.00007	3.337	0.020	60.2	25.6	64.51	0.89	
7	0.00517	0.00007	0.00000	0.00006	3.538	0.021	56.8	29.2	64.50	0.91	
8	0.00596	0.00024	0.00000	0.00025	3.673	0.071	52.1	7.1	61.41	2.35	
9	0.00892	0.00092	0.00000	0.00104	4.647	0.272	43.3	1.7	64.57	8.65	
10	0.00538	0.00027	0.00000	0.00033	3.611	0.081	56.0	5.4	64.86	2.65	
11	0.01602	0.00369	0.00000	0.00434	5.929	1.090	20.2	0.4	38.46	35.13	
12	0.04161	0.01318	0.00000	0.01464	12.952	3.902	5.1	0.1	20.97	126.99	
3–12								98.7	63.70	0.49	

Table 2. (Continued).

Step	BULG 82		J-value: <b>0.01832 ± 0.0001832</b>		amphibole	Velichkovo		% <sup>40</sup> Ar <sup>c</sup>	% <sup>39</sup> Ar	age [Ma]	±
	<sup>36</sup> Ar/ <sup>39</sup> Ar <sup>a</sup>	±	<sup>37</sup> Ar/ <sup>39</sup> Ar <sup>b</sup>	±		<sup>40</sup> Ar/ <sup>39</sup> Ar <sup>a</sup>	±				
1	0.02336	0.00155	23.15239	0.00173	8.855	0.459	22.1	0.3	120.64	14.24	
2	0.01742	0.00086	12.43288	0.00107	6.198	0.255	16.9	0.5	65.16	8.15	
3	0.00659	0.00026	0.73130	0.00030	5.462	0.078	64.3	1.7	113.87	2.65	
4	0.00577	0.00022	1.10714	0.00029	4.299	0.065	60.3	1.7	86.02	2.22	
5	0.00711	0.00021	1.63733	0.00020	4.380	0.063	52.0	2.4	77.32	2.12	
6	0.00476	0.00029	6.57552	0.00028	3.340	0.085	57.9	1.7	78.70	2.81	
7	0.00374	0.00013	2.75171	0.00012	3.343	0.039	66.9	4.1	78.80	1.46	
8	0.00295	0.00007	3.91591	0.00007	3.158	0.020	72.4	7.7	83.29	1.04	
9	0.00325	0.00002	5.88949	0.00002	3.003	0.007	68.0	26.5	80.46	0.82	
10	0.00248	0.00006	4.60451	0.00006	2.860	0.017	74.3	10.2	79.89	0.94	
11	0.00264	0.00006	4.30563	0.00006	2.917	0.018	73.3	9.3	79.50	0.97	
12	0.00270	0.00004	5.13549	0.00004	2.847	0.013	72.0	13.6	78.80	0.87	
13	0.00257	0.00026	4.83092	0.00023	2.859	0.077	73.4	2.1	79.60	2.56	
14	0.00218	0.00006	4.68276	0.00006	2.747	0.017	76.5	9.9	79.33	0.95	
15	0.00297	0.00013	7.71577	0.00013	2.830	0.038	69.0	4.2	82.15	1.45	
16	0.00341	0.00016	7.74488	0.00017	2.850	0.049	64.6	3.0	78.70	1.72	
17	0.00099	0.00055	24.60136	0.00064	3.234	0.163	90.9	0.8	154.94	5.16	
5–16								94.9	79.99	0.34	
Step	BULG 82		J-value: <b>0.01821 ± 0.0001821</b>		biotite	Velichkovo		% <sup>40</sup> Ar <sup>c</sup>	% <sup>39</sup> Ar	age [Ma]	±
	<sup>36</sup> Ar/ <sup>39</sup> Ar <sup>a</sup>	±	<sup>37</sup> Ar/ <sup>39</sup> Ar <sup>b</sup>	±		<sup>40</sup> Ar/ <sup>39</sup> Ar <sup>a</sup>	±				
1	0.005545	0.000179	3.116516	0.000197	4.777	0.053	65.7	1.6	107.42	1.94	
2	0.007095	0.000369	6.002325	0.000416	4.235	0.109	50.5	0.8	83.28	3.52	
3	0.003577	0.000127	1.686573	0.000127	3.413	0.037	69.0	2.4	79.46	1.41	
4	0.002314	0.000123	2.522986	0.000102	3.390	0.036	79.8	2.4	92.52	1.45	
5	0.002609	0.000070	1.976691	0.000051	3.018	0.021	74.5	4.7	76.77	1.00	
6	0.003970	0.000201	4.263496	0.000143	3.237	0.059	63.8	1.7	76.62	2.01	
7	0.002310	0.000105	1.457140	0.000106	3.066	0.031	77.7	2.5	79.78	1.25	
8	0.002668	0.000131	2.613781	0.000125	3.057	0.039	74.2	1.9	79.00	1.44	
9	0.002185	0.000074	1.429735	0.000074	2.919	0.022	77.9	3.5	76.23	1.02	
10	0.002491	0.000092	2.129134	0.000089	2.958	0.027	75.1	3.0	76.35	1.14	
11	0.000950	0.000050	0.000000	0.000060	2.720	0.015	89.7	5.6	77.91	0.89	
12	0.001380	0.000104	0.026833	0.000127	2.815	0.031	85.5	2.4	76.98	1.22	
13	0.000780	0.000040	0.283034	0.000048	2.635	0.012	91.3	6.5	77.53	0.85	
14	0.000886	0.000028	0.126833	0.000034	2.679	0.008	90.2	9.3	77.55	0.80	
15	0.000628	0.000034	0.000000	0.000025	2.641	0.010	93.0	10.1	78.42	0.83	
16	0.000762	0.000070	0.012258	0.000063	2.608	0.021	91.4	4.0	76.18	0.99	
17	0.000425	0.000052	0.048418	0.000056	2.606	0.015	95.2	5.4	79.33	0.91	
18	0.000709	0.000040	0.003674	0.000039	2.623	0.012	92.0	7.1	77.13	0.84	
19	0.000721	0.000035	0.091984	0.000031	2.634	0.010	91.9	8.8	77.57	0.83	
20	0.001191	0.000065	2.791571	0.000072	2.635	0.019	86.6	3.5	79.89	0.99	
21	0.001410	0.000056	2.679942	0.000062	2.611	0.017	84.0	4.1	76.84	0.92	
22	0.001990	0.000087	3.874900	0.000082	2.653	0.026	77.8	3.3	75.70	1.10	
23	0.001723	0.000065	4.334124	0.000066	2.604	0.019	80.4	3.7	77.79	0.97	
24	0.004747	0.000147	11.182587	0.000151	2.693	0.044	47.9	1.6	69.29	1.53	
5–23								91.2	77.58	0.23	

Errors of ratios, J-values and ages are at the 1-sigma level.

<sup>a</sup> Measured<sup>b</sup> Corrected for post-irradiation decay of <sup>37</sup>Ar<sup>c</sup> Non atmospheric <sup>40</sup>Ar

through ca. 500 °C after lava extrusion. It corresponds with recent time-scale calibration, which gives an age of 89.3 Ma for the Coniacian/Santonian boundary (Gradstein et al. 2004).

An experiment was performed on amphibole from an amphibole-bearing granitoid enclave (BULG-104) within trachyandesite. Steps 1–5 yielded extraneous argon with variable ages. Steps 6–14 yielded a plateau age of 77.79 ± 0.48 Ma constituting

together 87.1 percent of <sup>39</sup>Ar released (Fig. 5c). The significance of this age is uncertain.

An experiment was performed on amphibole from an amphibole-bearing andesite bomb (BULG-105) of the uppermost volcanic level. The first five steps yielded extraneous argon with variable ages. Steps 6–14 yielded a staircase pattern with three steps with a minimum age of 18.7 ± 3.6 Ma. This age is in-

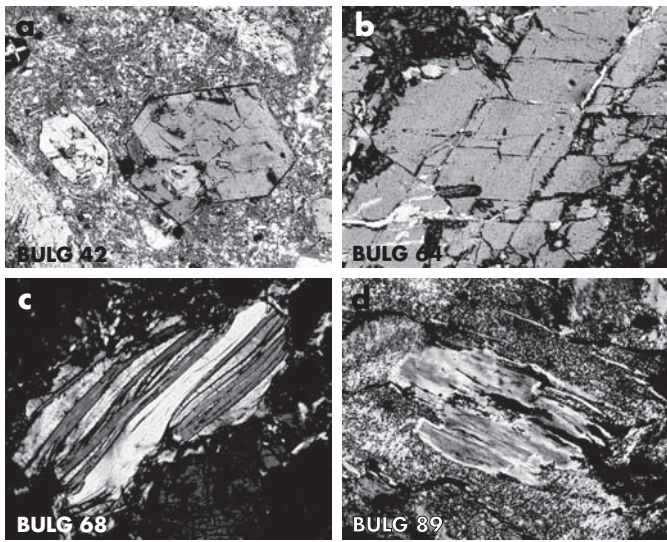


Fig. 3. Representative microfabrics of some samples with major importance for interpretation. (a) Amphibole from an andesite, sample BULG 42, Vozdol at Chelopech, (b) unaltered amphibole of sample BULG 64, Tolponitsa section. Width of section for (a) and (b) is 2 mm. (c) White mica in a crystal/lithic tuff, BULG 68, Tolponitsa section, (d) xenocrystic white mica grains in a dacitic andesite, sample 89, Elshitsa. Width of section for (c) and (d) is 1 mm.

terpreted to represent the maximum age of a low-temperature overprint. Steps 10–14 yield a plateau age of  $83.99 \pm 0.49$  Ma constituting together 91.2 percent of  $^{39}\text{Ar}$  released (Fig. 5d). Latter age represents the age of cooling through ca. 500 °C and the age of the lava. It is in line with the stratigraphic age as underlying marls were deposited at ca. the Santonian/Campanian boundary (83.5 Ma according to Gradstein et al. 2004). The

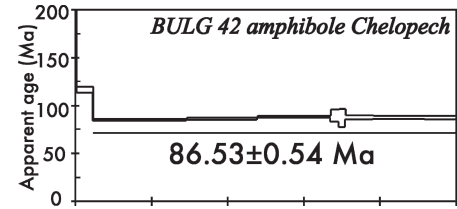


Fig. 4.  $^{40}\text{Ar}/^{39}\text{Ar}$  apparent age spectra of an amphibole multi-grain sample (ca. 10–20 grains) from a volcanic rock from Chelopech. Laser energy increases from left to right. Vertical width of bars represents  $1\sigma$  errors. Steps used for calculation of plateau ages are delineated by bar.

argon loss in the first increments can be explained by a loss due to a later, non-pervasive weak hydrothermal event.

The white mica concentrate from sample BULG-68 represents clasts within a lithic tuff (Fig. 3c) and could possibly date the source of the xenoliths. The resulting Ar isotopic release pattern shows a plateau age of  $313.0 \pm 1.1$  Ma constituting together 96.6 percent of  $^{39}\text{Ar}$  released (Fig. 5e). We suggest that this age represents the maximum age of cooling through ca. 350–400 °C after amphibolite-grade metamorphism in the source region. The age is similar to  $^{40}\text{Ar}/^{39}\text{Ar}$  white mica ages recently reported from the Srednogorie basement (Velichkova et al. 2004). The age also demonstrates that heating during magma ascent was unable to reset the argon isotopic system because of its short duration.

#### Sv. Nikola hill section

An experiment was performed on an amphibole concentrate from an amphibole-bearing granite (BULG-102) within an

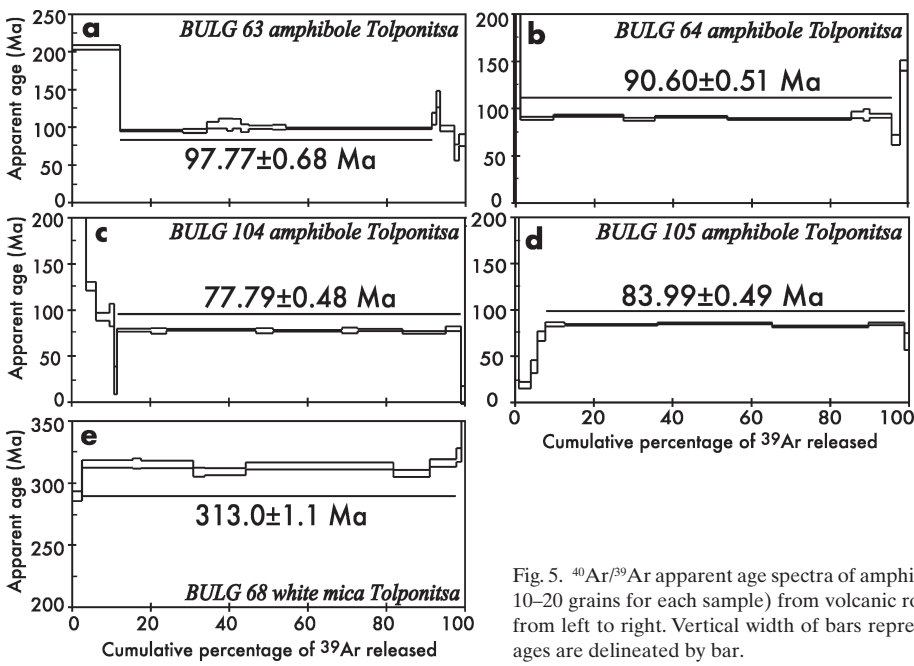


Fig. 5.  $^{40}\text{Ar}/^{39}\text{Ar}$  apparent age spectra of amphibole (a–d) and white mica (e) multi-grain samples (ca. 10–20 grains for each sample) from volcanic rocks of the Tolponitsa section. Laser energy increases from left to right. Vertical width of bars represents  $1\sigma$  errors. Steps used for calculation of plateau ages are delineated by bar.

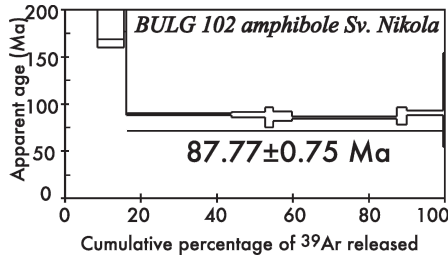


Fig. 6.  $^{40}\text{Ar}/^{39}\text{Ar}$  apparent age spectra of an amphibole multi-grain sample (ca. 10–20 grains) from a volcanic rock from Sv. Nikola hills. Laser energy increases from left to right. Vertical width of bars represents  $1\sigma$  errors. Steps used for calculation of plateau ages are delineated by bar.

andesite lava flow exposed ca. 1 km south of Sv. Nikola Hills. Steps 1–8 yielded extraneous argon. Steps 9–16 yielded a plateau age of  $87.77 \pm 0.75$  Ma constituting together 83.8 percent of  $^{39}\text{Ar}$  released (Fig. 6). The age, again, could represent the age of cooling through ca.  $500^\circ\text{C}$  or, more likely, the approximate age of argon loss.

#### Vlaykov Vruh

Sample BULG-84 from Vlaykov Vruh is a slightly altered porphyritic dacite. Results indicate a saddle-shaped pattern for the analysed amphibole (Fig. 7a). The first steps of  $^{39}\text{Ar}$  released yielded variable ages indicating some extraneous argon. Steps 4–11 yielded a plateau age of  $90.43 \pm 0.54$  Ma constituting together 91.2 percent of  $^{39}\text{Ar}$  released. This age represents the maximum age of cooling through ca.  $500^\circ\text{C}$ .

#### Plutonic rocks from Velichkovo

An experiment was performed on amphibole from the Velichkovo granodiorite (BULG-82). The first step of  $^{39}\text{Ar}$  released yielded some variable ages suggesting a small amount of extraneous argon (Fig. 7b). Steps 5–16 yielded a plateau age of  $79.99 \pm 0.34$  Ma constituting together 94.9 percent of  $^{39}\text{Ar}$  released. This age represents the maximum age of cooling through ca.  $500^\circ\text{C}$ .

A biotite concentrate from the same sample (BULG-82; Fig. 7c) displayed variable, higher ages at low-energy steps. Intermediate steps 5–23 of  $^{39}\text{Ar}$  released yielded a plateau age of  $77.58 \pm 0.23$  Ma constituting together 91.2 percent of  $^{39}\text{Ar}$  released. This age represents the maximum age of cooling through ca.  $300^\circ\text{C}$ .

#### Plutonic rocks from Elshitsa

Amphibole from a medium- to fine-grained unaltered granodiorite (BULG-88) from the dump near the shaft at Elshitsa yielded a disturbed saddle-shaped pattern (Fig. 8a). The first steps of  $^{39}\text{Ar}$  released yielded variable ages indicating some extraneous argon, respectively argon loss. Steps 7–13 yielded a plateau age of  $94.98 \pm 0.71$  Ma constituting together 77.2 per-

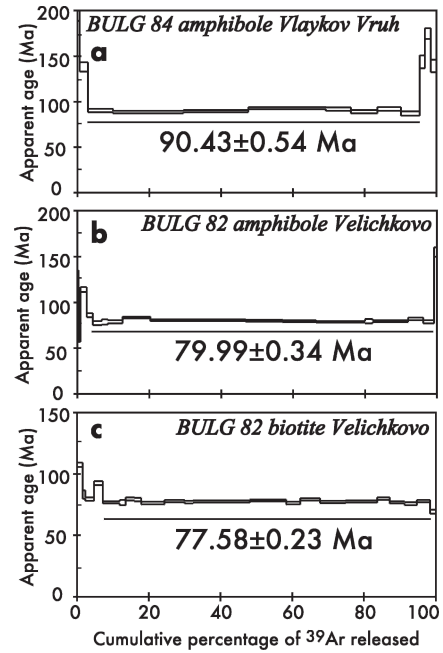


Fig. 7.  $^{40}\text{Ar}/^{39}\text{Ar}$  apparent age spectra of amphibole and biotite samples (ca. 10–20 grains for each sample) from plutonic rocks exposed at Vlaykov Vruh and Velichkovo. Laser energy increases from left to right. Vertical width of bars represents  $1\sigma$  errors. Steps used for calculation of plateau ages are delineated by bar.

cent of  $^{39}\text{Ar}$  released. High-energy release steps indicate some variable, higher ages. We suggest that the plateau age is likely geologically not significant. The true maximum age of cooling through ca.  $500^\circ\text{C}$  is expected to be slightly younger due to possible incorporation of extraneous argon.

The biotite concentrate from sample BULG-88 indicated also a saddle-shaped pattern with variable and higher ages at low- and high-energy steps (Fig. 8b). Intermediate steps 5–20 yielded a plateau age of  $86.84 \pm 0.29$  Ma constituting together 92.2 percent of  $^{39}\text{Ar}$  released. This age represents the maximum age of cooling through ca.  $300^\circ\text{C}$ .

An experiment was performed on a secondary white mica concentrate from a reddish altered dacitic andesite from the abandoned open pit at Elshitsa west. The rock contains 1–6 mm clusters of fine-grained granitoid xenoliths, within which biotite altered to white mica (BULG-89, Fig. 3d) with leucoxene/ore mineral exsolution. The resulting Ar isotopic release pattern shows low-energy steps with variable, higher ages. Steps 5–17 of  $^{39}\text{Ar}$  released yielded a plateau age of  $91.33 \pm 0.38$  Ma constituting together 88.9 percent of  $^{39}\text{Ar}$  released (Fig. 8c). This age represents the maximum age of cooling through ca.  $350$ – $400^\circ\text{C}$  after alteration.

A stepwise heating experiment was carried on sample BULG-101 from a chloritized amphibole-bearing Elshitsa granodiorite. Steps 3–12 on amphibole yielded a plateau age of  $63.70 \pm 0.49$  Ma constituting together 98.7 percent of  $^{39}\text{Ar}$  released (Fig. 8d). We suggest that this age indicates resetting during hydrothermal alteration. In thin-section, amphiboles of

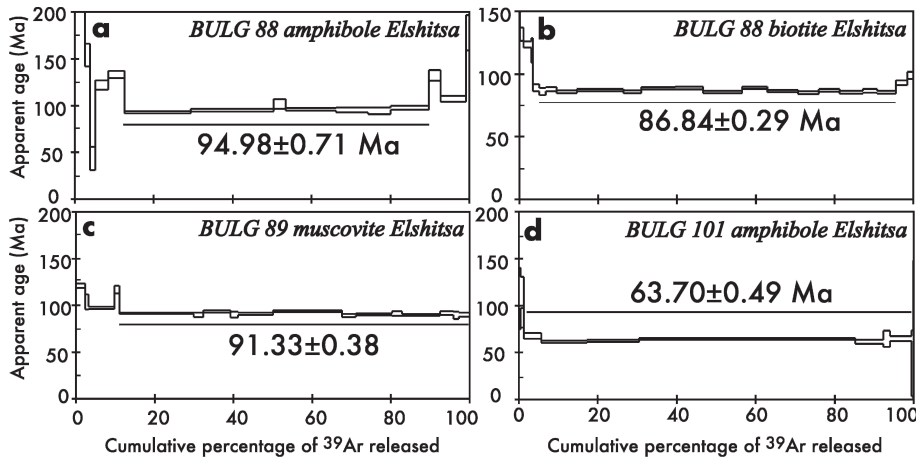


Fig. 8.  $^{40}\text{Ar}/^{39}\text{Ar}$  apparent age spectra of amphibole (a, c) and biotite (b) samples from Elshitsa granodiorite and white mica (d) multi-grain samples (ca. 10–20 grains for each sample) from a dacite. Laser energy increases from left to right. Vertical width of bars represents  $1\sigma$  errors. Steps used for calculation of plateau ages are delineated by bar.

this sample show some alteration rims and are rich in inclusions.

## Discussion

Most of our new  $^{40}\text{Ar}/^{39}\text{Ar}$  ages (Fig. 9) from magmatic rocks of the Panagyuriste ore region are in line with U-Pb zircon ages and recently reported  $^{40}\text{Ar}/^{39}\text{Ar}$  ages (e.g. von Quadt et al. 2002, 2003; Chambefort et al. 2003; Handler et al. 2004; Lips et al. 2004; for full references and data set, see Table 1). They extend the age range and allow the correlation of plutonic suites, from which nearly all previous age data were reported, with volcanic sequences and therefore also with biostratigraphy of intercalated sedimentary rocks.

The new  $^{40}\text{Ar}/^{39}\text{Ar}$  ages indicate that magmatic amphibole is highly accessible to secondary alteration, and seemingly relatively well-preserved amphiboles often date the maximum age of secondary alteration. The most extreme example is sample BULG 101 from Elshitsa with an age of  $63.70 \pm 0.49$  Ma. Peytcheva et al. (2007) found U-Pb zircon ages ranging from 90.5 to 89.3 Ma interpreted to represent magma crystallisation. Accepting this interpretation, several steps of secondary alteration might have occurred. The age is clearly younger than ore-forming alteration found in Chelopech (ca. 91–91.5 Ma; Chambefort et al. 2003) and in Medet (ca. 90.5–89.3 Ma; Peytcheva et al. 2007).

Magmatism in the Panagyurishte corridor was likely not continuous as also indicated by three major volcanic levels exposed in the southern Central Srednogorie basin (Fig. 9), e.g. along the Tolponitsa river. These include a group with ages between 91–90 Ma in the northernmost unit, then an age group at ca. 85–84 Ma and a final age group between 82 and 77 Ma. The latter group seems to be barren as the missing evidence of ore mineralization suggests.

The  $^{40}\text{Ar}/^{39}\text{Ar}$  age of 78–80 Ma for hydrothermal alteration and associated mineralization in the deposits Elatsite and Medet (Lips et al. 2004), however, is not consistent with U-Pb zircon dating in the Elatsite deposit, from which von Quadt et al. (2002) reported an age of 92–91 Ma. We suggest that the

$^{40}\text{Ar}/^{39}\text{Ar}$  white mica age of 78–80 Ma of Lips et al. (2004) indicates a stage of hydrothermal alteration but not necessarily of

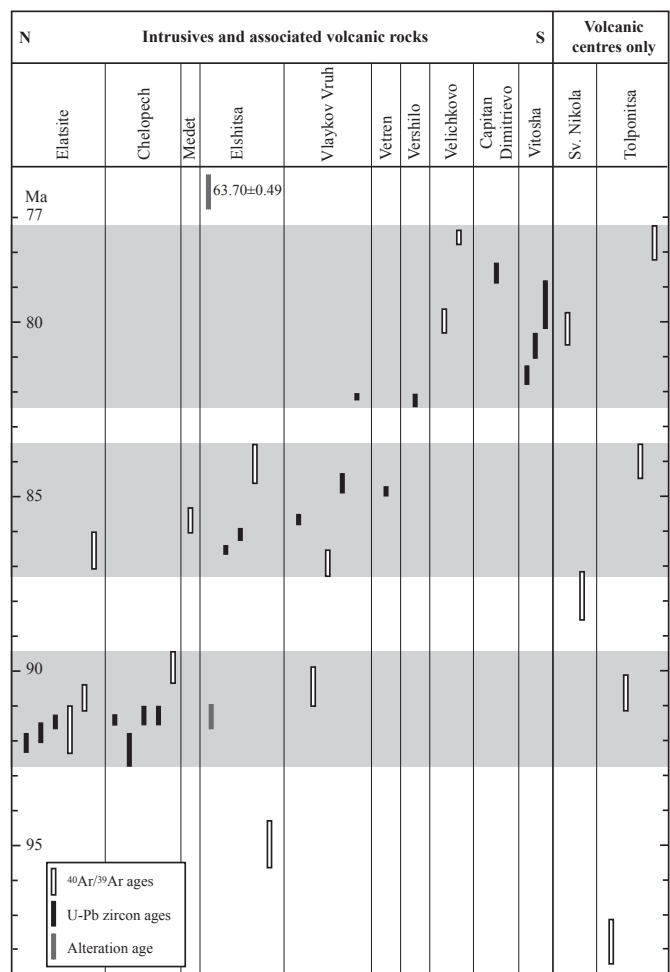


Fig. 9. Comparison of U-Pb zircon and  $^{40}\text{Ar}/^{39}\text{Ar}$  mineral ages of plutonic and volcanic rocks and alteration from the Panagyurishte region. For data sources, see Table 1 and results of this study. Grey bars indicate major volcanic levels, as discussed in the text.

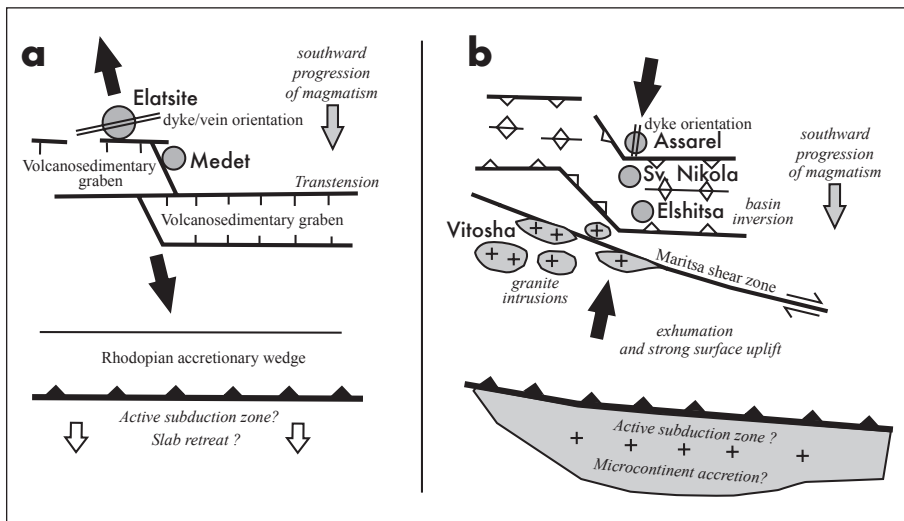


Fig. 10. Two-step tectonic model for the evolution of the Panagyurishte region (slightly modified after Handler et al. 2004). (a) Southward retreat of the subduction zone, (b) Accretion of a microcontinent to the subduction complex. See text for discussion.

mineralization. Our ages of possible alteration are also unrelated to mineralizing fluids. These ages vary and show, in combination with Lips et al. (2004) data, several stages of secondary overprint and alteration.

Late Cretaceous magmatism started earlier in Bulgaria than in Serbia and in Romania. In Serbia, U-Pb zircon and  $^{40}\text{Ar}/^{39}\text{Ar}$  ages range from ca. 86 to 78 Ma (Clark & Ullrich 2004; Stein et al. 2002; Lips et al. 2004). In Romania, high-precision U-Pb and Re-Os ages of ca. 76 Ma have been reported (Nicoleescu et al. 1999; Ciobanu et al. 2002) and recently, Wiesinger et al. (2007) found U-Pb zircon ages of ca. 79 Ma in one of the plutons of the Banat region (Romania), which are clearly younger than Late Cretaceous magmatism in Serbia and Bulgaria. This suggests a northward younging of Banatite magmatism along strike of the belt.

The cause of magmatism and accompanying processes, like formation of sedimentary basins, is still under debate. Two alternative models have been proposed, (1) northward subduction of Tethyan oceanic crust beneath Moesia and (2) post-collisional slab break-off (see Ciobanu et al. 2002; Neubauer 2002; von Quadt et al. 2005 and Chambefort & Moritz 2006 for discussion). We adopt here the model of Handler et al. (2004) and modify this according to further new structural data (Neubauer et al., unpublished results). In the subduction model, the southward shift of magmatism and sedimentary basin formation would be possibly triggered by a southward retreat of the subduction zone (Fig. 10a). Such a zone of continuous Late Cretaceous-Palaeogene accretion along a subduction zone was postulated for the Rhodopian metamorphic complex by Barr et al. (1999) and Krohe & Mposkos (2002), although no full evidence exists for Late Cretaceous, Turonian-Campanian, subduction. The subsequent change to N-S compression (during the 86–78 Ma period) could be explained by accretion of a microcontinent to the subduction complex, which exerted horizontal compressional forces perpendicular to the strike of

the continental margin (Fig. 10b). Adopting the slab break-off model, the change in palaeostress orientations can be explained in a similar way. The initial stage of slab break-off would have resulted in a short period of extension perpendicular to strike of the orogen. Subsequent shortening may have been driven by large-scale plate motion.

## Conclusions

The results allow drawing the following major conclusions:

- (1) The new  $^{40}\text{Ar}/^{39}\text{Ar}$  ages show the duration of intrusions of subvolcanic bodies and the volcanic surface expressions between ca. 94 and 78 Ma.
- (2) The data show a principal north-to-south progression of magmatism, crossing the main trend of the Banat-Srednogorie belt.
- (3) There are three distinct levels of volcanism within a volcano-sedimentary section, which show a punctuation of magmatism. The three distinct levels of magmatism are expressed in both plutonic and volcanic rocks.
- (4) Pre-Alpine  $^{40}\text{Ar}/^{39}\text{Ar}$  white mica ages of xenoliths seem to survive volcanic eruptions.
- (5) A change in the structural setting occurred between the 92–90 Ma and 86–78 Ma periods. In the earlier stage, N-S extension prevailed whereas in the second stage ca. N-S compression was predominant.

## Acknowledgements

This work has been carried out within the project P15.464-GEO of the Austrian Research Foundation. Jan Wijbrans and Kalin Kouzmanov helped with their constructive reviews to improve the manuscript.

## Appendix: Sample locations and descriptions

### Chelopech

**BULG-42:** Hornblende andesite. Vosdol valley, NE of Chelopech mine. Well-preserved andesite shows no alteration but abundant volcanic resorption phenomena. Greenish amphibole grains are 1–1.5 mm large and comprise a rim of clinopyroxene. Plagioclase grains are twinned, xenomorphic, show an optical zonation and are partly resorbed. Perthitic alkali feldspar grains and opaque minerals (0.05–0.1 mm) are rare. The microcrystalline groundmass is essentially composed of 0.01 to 0.05 mm large feldspar grains.

### Tolponitsa section

**BULG-63** (Hornblende): N 42° 36' 54.7", E 24° 01' 34.7". Tolponitsa River valley. Massive lava flow at the base of the section with relatively well preserved phenocrysts, dominantly plagioclase and rare opaque minerals, amphibole and clinopyroxene. Plagioclase is ca. 0.4 to 2 mm large, twinned, zoned and in part replaced by sericite. Alkali feldspar occurs in a few grains. Amphibole is greenish-brown and occurs in xenomorphic relics, without any inclusions. Some amphibole relics are mantled by clinopyroxene, which occurs otherwise in a few separate, well-preserved grains. Amphibole is always part of aggregates, including plagioclase, opaque minerals, epidote, calcite, sphene, apatite and very rare biotite. Opaque minerals form also separate aggregates with individual, xenomorphic ca. 0.1 mm large grains. The groundmass is fine-grained (ca. 0.01 mm) and comprises feldspar and subordinate chlorite.

**BULG-64** (Hornblende): N 42° 34' 49.7", E 24° 00' 26.6". Tolponitsa River valley, SE of Petrich. Coarse-grained biotite-bearing andesite crystal tuff with mm-sized amphiboles. Amphibole occurs in a few brownish, ca. 0.5–0.7 mm large well-preserved grains, that do not show any alteration. They are also nearly free of inclusions. Some clinopyroxene is common. Plagioclase grains are ca. 0.4–0.6 mm large and bear some serpentine aggregates in their cores. Opaques (ca. 0.1–0.2 mm in diameter) are xenomorphic, comprising a further important constituent. The devitrified groundmass comprises chlorite, serpentine and calcite as secondary minerals.

**BULG-68** (Muscovite): N 42° 32' 23.3", E 24° 00' 03.5". Tolponitsa River valley, road to Srebrinovo. Crystal/lithic tuff. Well-preserved resorbed quartz grains are ca. 0.5 mm large. Clinopyroxene is another unaltered component. Lithic clasts comprise quartz and sericite/muscovite. In contrast, feldspar is strongly altered into secondary sericite. Pseudomorphs (after olivine) composed of serpentine are common. Altered vitric volcanic clasts are rich in secondary sericite. Secondary minerals are chlorite, serpentine, sericite, subordinate calcite, and rare talc.

**BULG-104** (Hornblende): Tolponitsa River valley, ca. 3 km S of Petrich. Amphibole-bearing enclave in trachyandesite, ca. 60 cm below the base of marl. Trachyandesite with some significant alteration, which is distributed in patches. Brown-green idiomorphic or xenomorphic amphibole phenocrysts are 0.3 to 1.5 mm large, bear leucoxene/opaque along margins and have mostly no inclusions. They form aggregates, i.e. enclaves. Plagioclase is hypidiomorphic, twinned and in part replaced by sericite ± calcite. Apatite and hypidiomorphic opaque minerals (ca. 0.1–0.2 mm large) are further constituents. The groundmass comprises fine-grained plagioclase and alkali feldspar laths (ca. 0.07 mm long), which form a trachytic texture.

**BULG-105** (Hornblende): Tolponitsa River valley, ca. 3 km S of Petrich. Amphibole-bearing andesite bomb, ca. 60 cm below the base of marl. Lava with fine-grained microcrystalline, trachytic groundmass with plagioclase laths, which are ca. 0.05 mm long, and opaques and chlorite patches. Brownish amphibole is xenomorphic, poor in inclusions (opaques, quartz, alkali feldspar, plagioclase), but in part decomposed with K-feldspar along cleavage planes and comprises often rims of fine-grained opacitic minerals.

### Sv. Nikola hills

**BULG-102** (Hornblende): Ca. <1 km S of Sv. Nikola hills. Andesite with granodiorite xenoliths. The lava flow comprises amphibole, plagioclase and opaque phenocrysts. Amphibole is greenish and idiomorphic. Grains are 0.4 to 3 mm long. Small amphibole grains are poor in inclusions and bear sometimes opaque grains along their margins. Large grains have plagioclase and opaque inclusions, which are 0.03–0.05 mm large. Other minerals are hypidiomorphic opaque grains, apatite and rare epidote. The groundmass comprises fine-grained isometric feldspar (mostly plagioclase, 0.05 mm in diameter) and spherolitic textures (ca. 0.25 mm in diameter) with fibres of feldspar or chaledony.

### Elshitsa

**BULG-88** (Hornblende, Biotite): N 42° 21' 48.1", E 24° 12' 44.8". Elshitsa, sample from a late mining dump ca. 100 m SE of the shaft. Medium- to fine-grained unaltered Elshitsa granodiorite. Well-preserved, fully crystallized granodiorite with an average grain size of 1–2 mm. Quartz is skeletal and comprises alkali feldspar inclusions. Plagioclase is optically zoned, twinned and largely unaltered. Some alteration of plagioclase occurs only in the crystal centres. Alkali feldspar is perthitic. Greenish amphibole grains are well-preserved, and bear unaltered biotite inclusions and strongly sericitized feldspar inclusions. Brown amphibole is unaltered in most grains. Some other grains show small rims with alteration into chlorite and opaques. Isometric opaque minerals are hypidiomorphic and of magmatic origin.

**BULG-89** (Muscovite): N 42° 21' 47.5", E 24° 12' 14.1". Elshitsa west, abandoned open pit. Reddish altered dacitic andesite with white mica as an alteration product. Andesite with small (1–6 mm) granitoid xenoliths. The andesite comprises phenocrysts of the size 0.5 to 4 mm, including skeletal quartz and plagioclase laths. Plagioclase is twinned, hypidiomorphic to idiomorphic. Idiomorphic zones of sericitisation occur in the interior of plagioclase, but never along rims. Skeletal opaque minerals are rich in inclusions, round and isometric. Zircon is a further constituent. The groundmass comprises fine-grained (0.01–0.02 mm) quartz, feldspar and sericite. The granitoid xenoliths comprise plagioclase, alkali feldspar and large (0.4–2 mm) white mica grains. These white mica grains comprise leucoxene and opaque laths, suggesting the derivation of white mica from biotite.

**BULG-101** (Hornblende): Roadcut 1 km S of the abandoned quarry of Vlaykov Vruh. Chloritized Elshitsa monzonite (granodiorite according to geological map). The rock is fully crystallised and comprises ca. 0.5 mm large idiomorphic to hypidiomorphic, twinned plagioclase grains and large alkali feldspar grains. Clinopyroxene is in part decomposed to light-greenish amphibole. Skeletal, xenomorphic, light-greenish amphibole grains form big, up to 10 mm large crystals, which are full of inclusions of plagioclase, pseudomorphs with chlorite, and aggregates of clinopyroxene and fine-grained opaque minerals. Along amphibole margins the colour changes to light-greenish. Further primary magmatic minerals are opaques. Secondary minerals are calcite and clinozoisite.

### Velichkovo

**BULG-82** (Biotite, Hornblende): N 42° 15' 37.5", E 24° 12' 54.1". Ca. 1 km NW Velichkovo, old quarry. Velichkovo granodiorite. Biotite is ca. 1.5 mm large, brown and sometimes in part replaced within a small zone by green biotite and leucoxene, respectively a mixture of fine-grained green biotite (0.05–0.1 mm) and opaque minerals. Some brown biotite grains display a sagenite network. Phenocystic quartz grains are up to 5 mm large. Plagioclase grains are 0.5–2 mm large and display a strong zoning. The cores are in part replaced by a mixture of sericite and epidote. Along plagioclase rims fine green biotite occurs sometimes. Alkali feldspars are perthitic or, in a few grains, microcline. Pseudomorphs are either composed of green biotite and subordinate (ca. 10 percent) epidote, or chlorite and epidote. Aggregates of isometric opaque minerals are common.

**BULG-84** (Hornblende): N 42° 21' 01.5", E 24° 13' 00.1". Vlaykov Vruh, southern side of the abandoned quarry. Slightly altered porphyritic dacite. Note: there is no amphibole visible in the thin section. Large, skeletal quartz phenocrysts. Hypidiomorphic plagioclase occurs in single grains or aggregates. Idiomorphic (ca. Hexagonal) pseudomorphs include either only epidote, or a mixture of epidote, chlorite and sphene/leucoxene. The groundmass displays a graphic texture of quartz and feldspar. Secondary minerals are fine-grained and comprise chlorite, sericite and epidote (max. 0.1 mm long).

## REFERENCES

- Aiello, E., Bartolini, C., Boccaletti, M., Gocev, P., Karagjuleva, J., Kostadinov, V. & Manetti, P. 1977: Sedimentary features of the Srednogorie zone (Bulgaria), an Upper Cretaceous intra-arc basin. *Sedimentary Geology* 19, 39–68.
- Arnaudov, V., Amov, B., Bratnitzkii, B. & Pavlova, M. 1989: Isotopic geochronology of magmatic and metamorphic rocks from Balkanides and Rhodope massif. XIV – Congress of CBGA, Sofia, sept., 1989, 1154–1157 (in Russian).
- Atanassova-Vladimirova, S., Mavrudchiev, B., von Quadt, A., Peytcheva, I. & Goergiev, S. 2004: Petrology and geochemistry of lamprophyric dykes in the Vitosha pluton. Proceedings of the Annual Scientific Conference, Bulgarian Geological Society, Sofia, Bulgaria, pp. 100–102.
- Barr, S. R., Temperley, S. & Tarney, J. 1999: Lateral growth of the continental crust through deep level subduction-accretion: arc-evaluation of central Greek Rhodope. *Lithos* 46, 69–94.
- Berza, T., Constantinescu, E. & Vlad, S. N. 1998: Upper Cretaceous magmatic series and associated mineralisation in the Carpathian-Balkan Orogen. *Resource Geology* 48, 291–306.
- Boccaletti, M., Manetti, P. & Peccerillo, A. 1974: The Balkanids as an instance of Back-Arc Thrust Belt: Possible relation with the Hellenids. *Geological Society of America Bulletin* 85, 1077–1084.
- Boccaletti, M., Manetti, P., Peccerillo, A. & Stanisheva-Vasilieva, G. 1978: The Late Cretaceous high-potassium volcanism in eastern Srednogorie, Bulgaria. *Geological Society of America Bulletin* 89, 439–447.
- Burg, J.P., Ivanov, Z., Ricou, L.E., Dimov, D. & Klain, L. 1990: Implication of shear-sense criteria for the tectonic evolution of the Central rhodope massif, southern Bulgaria. *Geology* 18, 451–454.
- Burg, J.P., Ricou, L., Ivanov, Z., Godfriaux, I., Dimov, D. & Klain, L. 1993: Crustal-scale thrust complex in the Rhodope massif. Structure and kinematics. *Bulletin of the Geological Society of Greece XXVIII*, 71–85.
- Chambefort, I., von Quadt, A. & Moritz, R. 2003: Volcanic environment and geochronology of the Chelopech high-sulfidation epithermal deposit, Bulgaria: regional relationship with associated deposits. European Union of Geosciences 12<sup>th</sup> Biennial Meeting, Nice, France, 6–11 April 2003. Abstract on CD: EAE03-A-00569.
- Chambefort, I. & Moritz, R. 2006: Late Cretaceous structural control and Alpine overprint of the high-sulfidation Cu-Au epithermal Chelopech deposit, Srednogorie belt, Bulgaria. *Mineralium Deposita* 41, 259–280.
- Channell, J.E.T. & Kozur, H. 1997: How many oceans? Meliata, Vardar, and Pindos oceans in Mesozoic Alpine paleogeography. *Geology* 25, 183–186.
- Ciobanu, C.L., Cook, N.G. & Stein, H. 2002: Regional setting and geochronology of the Late Cretaceous Banatic Magmatic and Metallogenic Belt. *Mineralium Deposita* 37, 541–567.
- Clark, A.H. & Ullrich, D. 2004:  $^{40}\text{Ar}/^{39}\text{Ar}$  age data for andesitic magmatism and hydrothermal activity in the Timok Massif, eastern Serbia: implications for metallogenetic relationships in the Bor copper-gold subprovince. *Mineralium Deposita* 39, 256–262.
- Cotta, B. von 1864: Über Eruptivgesteine und Erzlagerstätten in Banat und Serbien. Edit. V. Braunmüller, Wien, 105 pp.
- Csontos, L. & Vörös, A. 2004: Mesozoic plate tectonic reconstruction of the Carpathian region. *Palaeogeography, Palaeoclimatology, Palaeoecology* 210, 1–56.
- Foose, R.M. & Manheim, F. 1975: Geology of Bulgaria. *Amer. Assoc. Petrol. Geol. Bull.* 59, 303–335.
- Gradstein, F.M., Ogg, J.G. & Smith, A.G. (Eds.). 2004: A geologic time scale 2004. Cambridge University Press, Cambridge, 610 pp.
- Handler, R., Neubauer, F., Velichkova, S.H. & Ivanov, Z. 2004:  $^{40}\text{Ar}/^{39}\text{Ar}$  age constraints on the timing of magmatism and cooling in the Panagyurishte region, Bulgaria. *Schweizerische Mineralogische und Petrographische Mitteilungen* 84, 119–132.
- Heinrich, C.A. & Neubauer, F. 2002: Cu-Au(-Pb-Zn-Ag) metallogeny of the Alpine-Balkan-Carpathian-Dinaride geodynamic province: introduction. *Mineralium Deposita* 37, 533–540.
- Jankovic, S. 1997: The Carpatho-Balkanides and adjacent area: a sector of the Tethyan Eurasian metallogenic belt. *Mineralium Deposita* 32, 426–433.
- Kamenov, B., von Quadt, A. & Peytcheva, I. 2002: New insight into petrology, geochemistry and dating of the Vejen pluton, Bulgaria. *Geokhimiya, Mineralogiya i Petrologiya*, Sofia 39, 3–25.
- Karagjuleva, J., Kostadinov, V., Tzankov, Tz. & Gocev, P. 1974: Structure of the Panagyuriste strip east of the Topolnitsa river. *Bulletin of the Geological Institute*, ser. *Geotectonics* 13, 231–301.
- Krohe, A. & Mposkos, E. 2002: Multiple generations of extensional detachments in the Rhodope Mountains (northern Greece): evidence of episodic exhumation of high-pressure rocks. In: Blundell, D.J., Neubauer, F. & von Quadt, A. (Eds.): The timing and location of major ore deposits in an evolving orogen. *Geological Society of London Special Publication* 204, 151–178.
- Lilov, P. & Chipchakova, S. 1999: K-Ar dating of the Late Cretaceous magmatic rocks and hydrothermal metasomatic rocks from Central Srednogorie. *Geokhimiya, Mineralogiya i Petrologiya*, Sofia 36, 77–91.
- Lilov, P. & Stanisheva-Vassileva, G. 1998: Excess  $^{40}\text{Ar}$ ,  $^{87}\text{Sr}/^{86}\text{Sr}$  and K-Ar dating of minerals and rocks from the Tamarino paleovolcano: Sofia, Bulgaria. *Geokhimiya, Mineralogiya i Petrologiya*, Sofia 33, 61–72.
- Lips, A.L.W., Herrington, R.J., Stein, G., Kozelj, D., Popov, K. & Wijbrans, J.R. 2004: Refined timing of porphyry copper formation in the Serbian and Bulgarian portions of the Cretaceous Carpatho-Balkan belt. *Economic Geology* 99, 601–609.
- Liu, Y., Genser, J., Handler, R., Friedl, G. & Neubauer, F. 2001:  $^{40}\text{Ar}/^{39}\text{Ar}$  muscovite ages from the Penninic/Austroalpine plate boundary, eastern Alps. *Tectonics* 20, 528–547.
- Ludwig, K. R. 2001: IsoPlot/Ex – A Geochronological Toolkit for Microsoft Excel. Berkeley Geochronological Center Special Publication No. 1a.
- McDougall, I. & Harrison, M.T. 1999: *Geochronology and Thermochronology by the  $^{40}\text{Ar}/^{39}\text{Ar}$  Method*. 2<sup>nd</sup> ed, Oxford University Press, Oxford, 269 pp.
- Minkovska, V., Peybernès, B., Nikolov, T. and Ivanov, M. 2002: Paleogeographic reconstruction of a segment of the North-Tethyan margin in Bulgaria from Barremian to Albian. *Eclogae Geologicae Helvetiae* 95, 183–195.
- Moev, M. & Antonov, M. 1978: Stratigraphy of the Upper Cretaceous in the eastern part of Strelcha – Chelopech line. *Annuaire de l'Ecole Supérieure des Mines et de la Géologie*, Sofia 23, 7–30 (in Bulgarian with English Abstract).
- Moritz, R., Kouzmanov, K. & Petrunov, R. 2004: Late Cretaceous Cu-Au epithermal deposits of the Panagyurishte district, Srednogorie zone, Bulgaria. *Schweizerische Mineralogische und Petrographische Mitteilungen* 84, 79–99.
- Nachev, I. K. 1993: Late Cretaceous paleogeodynamics of Bulgaria. *Geologica Balcanica* 23, 3–23.
- Neubauer, F. 2002: Contrasting Late Cretaceous to Neogene ore provinces in the Alpine-Balkan-Carpathian-Dinaride collision belt. In: Blundell, D.J., Neubauer, F. & von Quadt, A. (Eds.): The timing and location of major ore deposits in an evolving orogen. *Geological Society of London Special Publication* 204, 81–102.
- Neugebauer, J., Greiner, B. & Appel, E. 2001: Kinematics of Alpine-West Carpathian orogen and palaeogeographic implications. *Journal of the Geological Society of London* 158, 97–110.
- Nicolescu, S., Cornell, D.H. & Bojar, A.V. 1999: Age and tectonic setting of the Ocna de Fier-Dogenecea skarn deposit, SW Romania. In: Stanley et al. (Eds.): *Mineral Deposits: Processes to Processing*. Balkema, Rotterdam, 1279–1282.

- Okay, A. I., Satir, M., Tüysüz, O., Akyüz, S. & Chen, F. 2001: The tectonics of the Strandja Massif: late Variscan and mid-Mesozoic deformation and metamorphism in the northern Aegean. *International Journal of Earth Science* 90, 217–233.
- Peytcheva, I. & von Quadt, A. 2003: U-Pb-zircon isotope system in mingled and mixed magmas: an example from Central Srednogorie, Bulgaria. *Geophysical Research Abstracts*, Vol. 5, 09177, Nice, electronic version.
- Peytcheva, I., von Quadt, A., Kamenov, B., Ivanov, Z.H. & Georgiev, N. 2001: New isotope data for Upper Cretaceous magma emplacement in the Southern and South-Western parts of Central Srednogorie. ABCD-GEODE Workshop, Vata Bai, Romania 79 suppl. 2, 82–83.
- Peytcheva, I., von Quadt, A., Kouzmanov, K. & Bogdanov, K. 2003: Elshitsa and Vlaykov Vruh epithermal and porphyry Cu (-Au) deposits of Central Srednogorie, Bulgaria: source and timing of magmatism and mineralization. In: Eliopoulos et al. (Eds.): *Mineral exploration and sustainable development*. Millpress, Rotterdam, 371–373.
- Peytcheva, I., von Quadt, A., Heinrich, C.A., Nedialkov, R., Neubauer, F., Moritz, R. 2007: Medet and Assarel Cu-porphyry deposits in Central Srednogorie; SE Europe: were they a common magmatic and hydrothermal system? In: Andrews, C.J. et al. (Eds.): *Proceedings of the Ninth Biennial SGA Meeting*, Dublin 2007, Volume 2, 881–884.
- Popov, P. 1987: Tectonics of the Banat-Srednogorie Rift. *Tectonophysics* 143, 209–216.
- Popov, P. 1996: On the tectono-metallogenic evolution of the Balkan peninsula alpides. UNESCO – IGCP project No 356 1, 5–17.
- Popov, P. & Popov, K. 1997: Metallogeny of Panagyurishte ore region. In: Romic, K. & Kondzulovic, R. (Eds.): *Proceedings of Ore Deposits Exploration*, Belgrade, April 2–4, 1997, Yugoslavia, 327–338.
- Popov, P. & Popov, K. 2000: General geologic and metallogenic features of the Panagyurishte ore region. In: Strashimirov, S. & Popov, P. (Eds.): *Geology and metallogeny of the Panagyurishte ore region (Srednogorie zone, Bulgaria)*. Guide to Excursions A and C. ABCD-GEODE 2000 Workshop, Borovets, Bulgaria, 1–7.
- Quadt, A. von, Peytcheva, I., Kamenov, B., Fanger, L. & Heinrich, C.A. 2002: The Elatitse porphyry copper deposit of the Panagyurishte ore district, Srednogorie zone, Bulgaria: U-Pb zircon geochronology and isotope-geochemical investigations of ore genesis. In: Blundell, D., Neubauer, F. & von Quadt, A. (Eds.): The timing and location of major ore deposits in an evolving orogen. *Geological Society of London Special Publication* 204, 119–135.
- Quadt, A. von, Peytcheva, I. & Cvetkovic, V. 2003: Geochronology, geochemistry and isotope tracing of the Cretaceous magmatism of East-Serbia and Panagyurishte district (Bulgaria) as part of the Apuseni-Timok-Srednogorie metallogenic belt in Eastern Europe. In: Eliopoulos et al. (Eds.): *Mineral exploration and sustainable development*. Millpress, Rotterdam, 407–410.
- Quadt, A. von, Moritz, R., Peytcheva, I. & Heinrich, C.A. 2005: Geochronology and geodynamics of Late Cretaceous magmatism and Cu-Au mineralization in the Panagyurishte region of the Apuseni-Banat-Timok-Srednogorie belt, Bulgaria. *Ore Geology Reviews* 27, 95–126.
- Renne, P.R., Swisher, C.C., Deino, A.L., Karner, D., Owens, T. & de Paolo, D. 1998: Intercalibration of standards, absolute ages and uncertainties in  $^{40}\text{Ar}/^{39}\text{Ar}$  dating. *Chemical Geology* 145, 117–152.
- Ricou, L.E., Burg, J.P., Godfriaux, I. & Ivanov, Z. 1998: Rhodope and Vardar: the metamorphic and the olistostromic paired belts related to the Cretaceous subduction under Europe. *Geodinamica Acta* 11, 285–309.
- Stampfli, C.M. & Mosar, J. 1999: The making and becoming of Apulia. *Memoire di Scienze Geologiche* 51, 141–154.
- Steiger, R. H. & Jäger, E. 1977: Subcommission on geochronology: Convention on the use of decay constants in geo- and cosmochronology. *Earth and Planetary Science Letters* 36, 359–362.
- Stein, G., Kozelj, D., Lips, A.L.W. & Bailly, L. 2002: The Timok magmatic complex (Serbia), an adakitic related magmatic event: *Geology and Metallogeny of Copper and Gold Deposits in the Bor Metallogenic Zone*. Symposium, Bor, Yugoslavia, October 24–25, 2002, Proceedings, 133–137.
- Stoykov, S. & Pavlishina, P. 2003: New data for Turonian age of the sedimentary and volcanic succession in the southeastern part of the Etrepole Stara Planina Mountain, Bulgaria. *Comptes Rendues de l'Académie Bulgare des Sciences* 56, 55–60.
- Stoykov, S., Peytcheva, I., von Quadt, A., Moritz, R., Yanev, Y. & Fontignie, D. 2004: Timing and magma evolution of the Chelopech volcano (Bulgaria). *Schweizerische Mineralogische und Petrographische Mitteilungen* 84, 101–118.
- Strashimirov, S. & Popov, P. 2000: Geology and metallogeny of the Panagyurishte ore region (Srednogorie zone, Bulgaria). ABCD-GEODE 2000 Workshop, Borovets, Guide to Excursions (A and C), Sofia, 52 pp.
- Velichkova, S., Handler, R. & Neubauer, F. 2001: Preliminary  $^{40}\text{Ar}/^{39}\text{Ar}$  mineral ages from the Central Srednogorie Zone, Bulgaria: Implications for Cretaceous geodynamics. *Romanian Journal of Mineral Deposits* 79, 112–113.
- Velichkova, S.H., Handler, R., Neubauer, F. & Ivanov, Z. 2004: Variscan to Alpine tectonothermal evolution of the Central Srednogorie Zone, Bulgaria: constraints from  $^{40}\text{Ar}/^{39}\text{Ar}$  analysis. *Schweizerische Mineralogische und Petrographische Mitteilungen* 84, 133–151.
- Wiesinger, M., Neubauer, F., Peytcheva, I., von Quadt, A., Berza, T. 2007: The Surduc pluton (Upper Cretaceous), Romania: significance for Banatite magmatism. In: Andrews, C.J. et al. (Eds.): *Proceedings of the Ninth Biennial SGA Meeting*, Dublin 2007, Volume 2, 913–916.
- Wijbrans, J.R., Pringle, M.S., Koopers, A.A.P. & Schveers, R. 1995: Argon geochronology of small samples using the Vulkaan argon laserprobe. *Proceedings Koninklijke Nederlandse Akademie van Wetenschappen* 98, 185–218.
- Willingshofer, E., Neubauer, F. & Cloetingh, S. 1999: Significance of Gosau basins for the upper Cretaceous geodynamic history of the Alpine—Carpathian belt. *Physics and Chemistry of the Earth Part A: Solid Earth and Geodesy* 24, 687–695.

Manuscript received January 4, 2007

Revision accepted October 4, 2007

Published Online first November 30, 2007

Editorial handling: U. Schaltegger